

**Functional Relevance of N-myristoyltransferase as a Biomarker for
Colorectal Cancer**

By

Tharmini Jenny Rathinagopal

Supervisor: Dr. Anuraag Shrivastav

A thesis submitted to the Faculty of Graduate Studies

The University of Winnipeg

in partial fulfillment of the requirements for the award of

Master of Science

Department of Biology

The University of Winnipeg

Manitoba, Canada, 2018

Abstract

Colorectal cancer (CRC) is the second leading cause of cancer deaths in Canada. The high mortality rate for CRC patients demonstrate the urgent need for a convenient, accurate and cost-effective screening test, which could triage patients for more intensive procedures such as colonoscopy. Current CRC screening tests are limited by their efficacy, invasiveness, and poor acceptability by the patients. N-myristoylation refers to the covalent attachment of the 14-carbon fatty acid myristoyl group to the N-terminal glycine residue of a target protein, which ensures its proper functioning and intracellular trafficking. This reaction is common amongst signalling proteins and is often integral to their activity. Myristoylation is catalyzed by N-myristoyltransferase which transfers the myristoyl moiety from myristoyl-coenzyme A to the N-terminal glycine residue.

The foremost aim of my study was to optimize and quantify *NMT1* and *METAP2* gene expression by using quantitative Polymerase Chain Reaction (qPCR). Due to its capacity to generate both qualitative and quantitative results, qPCR is considered a quick and accurate technique to begin with. *NMT1* and *METAP2* oncogenes overexpressed in colorectal cancer cells are directly associated with aggressive clinical behaviour. The *NMT1* and *METAP2* oncogenes and their respective protein products (NMT1 and METAP2) have been utilized for disease diagnosis and as predictive markers for treatment. To support accurate quantification and analysis in this study, I have optimized and standardized qPCR analysis to analyze colorectal cancer samples, obtaining significant and clinically useful results. We recently demonstrated that *NMT1* is expressed in the peripheral blood mononuclear cells (PBMC) and T cells of colorectal cancer patients. The aims of this study are to quantify *NMT1* and *METAP2* expression in

individuals undergoing colonoscopy and determine whether *NMT1* and *METAP2* gene expression could serve as a screening marker for CRC.

Chapter two: From chapter 1, it was determined that *NMT1* and *METAP2* expressions in peripheral blood and PBMC are potential biomarkers for CRC screening. These biomarkers are overexpressed in individuals with polyps and CRC. To understand the mechanism and the functional relevance of *NMT1* and *METAP2* overexpression in PBMC, *Nmt1* was knocked out in mouse embryonic stem cells and its effect was investigated on metabolic pathway. The generation of homozygous (*Nmt1*^{-/-}) deficient embryonic stem cells was confirmed by qPCR and Western analysis. The depletion of NMT1 leads to enhanced phosphorylation of key proteins within the PI3K/Akt signalling pathway that are normally stimulated by insulin and inhibited by rapamycin. The *Nmt1*-deficiency resulted in the over activation of the PI3K/Akt signalling pathway and *Igf1r* gene expression, thus, NMT1 likely has a vital role in regulating metabolic disorders.

Acknowledgement

Completion of this project would not be possible without the aid and support of the following people. They have contributed a great deal of time and dedication in helping me complete my research.

I would like to express my deepest and most sincere gratitude to my supervisor, Dr. Anuraag Shrivastav, for giving me the opportunity to complete my MSc thesis under his supervision. Thank you for all the advice, ideas, moral support and patience in guiding me through this project. I have been extremely lucky to have a supervisor who cared so much about my work. I would also like to thank my committee members Dr. Shailly Varma Shrivastav, Dr. Jens Franck, and Dr. Jude Uzonna. Their vast and impeccable knowledge in the field of molecular cell biology and their guidance is inspiring. Thank you for giving me the opportunity to grow in this field of research.

The success of this study required the help of all of my lab members and friends from the University of Winnipeg, Thank you for your encouragement and unconditional support throughout the entirety of my project. A special thank you to my dear friend Dr. Shiby for her continued support and kindness. Dr. Shiby Kuriakose was of great help to me as I balanced my research and my pregnancy, and I am grateful for her selflessness.

I would especially like to thank Dr. Harminster Singh and the nurses in the endoscopy unit at the Health Science Center. You were all very gracious and helpful when I recruited patients and collected data for my research. Thank you to all the participants in my research.

A special thanks to my family. Words cannot express how grateful I am to my father, mother, and siblings for the sacrifices that they've made on my behalf. Your devotion, unconditional love, patience, optimism, and advice were more valuable than you could ever imagine. I must express my gratitude to my beloved husband, Dr. Arasakumar Thangaraj. Thank you for supporting me in every way possible, and for the endless encouragement and love you have given me throughout this experience.

Table of Contents

Abstract.....	III
Acknowledgement	V
Table of Contents.....	VIII
List of Figures.....	X
List of Appendices	XIII
List of Abbreviations	XIV
CHAPTER 1: N-myristoyltransferase 1 and Methionine Aminopeptidase 2 are novel biomarkers for early detection of colorectal adenomatous polyps and cancers.....	1
Colorectal Cancer.....	1
N-myristoyltransferase (NMT) and Myristoylation.....	3
NMT and METAP2	3
Whole Blood.....	7
Peripheral Blood Mononuclear Cell (PBMC).....	7
HYPOTHESIS	9
OBJECTIVE	9
MATERIALS AND METHODS.....	10
Whole blood study: RNA isolation with PAXgene® kit.....	10
PBMC study: RNA isolation using Ficoll-Hypaque gradient centrifugation	10
RNA Quantification	11
cDNA Synthesis: Reverse Transcription of mRNA	11
Primers	11
Real Time Quantitative RT-PCR Analysis.....	11
Calculation of the amounts of gene expression	12
RESULTS	13
1. <i>NMT1</i> and <i>METAP2</i> gene expression in Whole Blood	13
2. <i>NMT1</i> and <i>METAP2</i> gene expression in PBMC.....	15

DISCUSSION	18
CHAPTER 2:	22
Functional Relevance of N-myristoyltransferase 1 in Cellular Growth Pathway.....	22
Mouse Embryonic Stem Cells	22
NMT and ESC.....	22
PI3K/Akt/mTOR Signaling Pathway.....	24
NMT Activity in PI3K/Akt/mTOR pathway	27
Rapamycin Treatment.....	27
HYPOTHESIS	30
OBJECTIVE	30
MATERIALS AND METHODS.....	31
ESC Cell culture	31
Western Blotting's	32
RESULTS	34
1. NMT1 protein expression is completely abrogated in <i>Nmt1</i> ^{-/-} ESC	34
2. PI3K p110 α expression is up-regulated in <i>Nmt1</i> ^{-/-} ESC.....	34
3. Akt phosphorylation is up regulated in <i>Nmt1</i> ^{-/-} ES cells compared to WT ESC	36
4. GSK phosphorylation is up regulated in <i>Nmt1</i> ^{-/-} ES cells compared to WT ESC	37
5. mTOR phosphorylation is up regulated in <i>Nmt1</i> ^{-/-} ES cells compared to WT ESC	38
6. <i>Nmt1</i> ^{-/-} ES cells show increased IGF1R phosphorylation compared to WT ESC	38
7. AMPK phosphorylation is upregulated in WT cells compared to <i>Nmt1</i> ^{-/-} ESC	40
DISCUSSION	41
CONCLUSION.....	43
REFERENCE.....	45
APPENDICES	50

List of Figures

Figure 1. Photographs showing normal, non-adenomatous polyp (NAP), adenomatous polyp (AP), and CRC colon.	2
Figure 2. Myristoylation reaction catalyzed by N-myristoyltransferase (NMT). The myristoyl functional group is added to the N-terminal glycine residue co-translationally following the removal of the N-terminal methionine residue by methionine aminopeptidase (MetAP) and the synthesis of myristoyl-CoA by acyl-CoA synthetase.	6
Figure 3. Isolation of PBMC by Ficoll-Paque density gradient centrifugation: The bottom layer is made up of red blood cells (erythrocytes) collected or aggregated by the Ficoll medium and sink completely through to the bottom. The next layer up from the bottom is primarily granulocytes, which also migrate down through the Ficoll-Paque solution. The next layer towards the top is the PBMC, which are typically at the interface between the plasma and the Ficoll solution, along with monocytes and platelets. To recover the PBMC, this layer is carefully recovered, washed with a HBSS to remove platelets, Ficoll, and plasma, then centrifuged again.	8
Figure 4. First set: Transcript levels of <i>NMT1</i> and <i>METAP2</i> from whole blood (PAXgene Tube), where Log ₂ (Fold change) expression values shown on y-axis are calculated relative to <i>GAPDH</i> and <i>ACTB</i> . Control (C), non-adenomatous polyps (P), adenomatous polyps (AP), and CRC patients are shown on x-axis.	14
Figure 5. Second set: Transcript levels of <i>NMT1</i> and <i>METAP2</i> from whole blood (PAXgene Tube), where Log ₂ (Fold change) expression values shown on y-axis are calculated relative to <i>ACTB</i> . Control (C), non-adenomatous polyps (P), adenomatous polyps (AP), and CRC patients are shown on x-axis.	14

Figure 6. Transcript levels of *NMT1* and *METAP2* from whole blood (PAXgene Tube), where Log 2 (Fold change) expression values shown on y-axis are calculated by relative to the average housekeeping genes: *GAPDH* and *ACTB*. Control, non-adenomatous polyps, adenomatous polyps, and CRC patients are shown on x-axis. *NMT1* and *METAP2* expression was lowest in adenomatous patients; however, *NMT1* and *METAP2* was the highest in non-adenomatous polyp and CRC patients. *METAP2* was significantly higher than *NMT1* in CRC patients' whole blood sample. 15

Figure 7. First set: Transcript levels of *NMT1* and *METAP2* in PBMC isolated from whole blood sample using density gradient centrifugation (Ficoll), where Log 2 (fold change) expression values shown on y-axis are calculated relative to the *GAPDH*. Control (C), non-adenomatous polyps (P), adenomatous polyps (AP), and CRC patients are shown on x-axis. *METAP2* and *NMT1* was significantly lower in control patients. 16

Figure 8. Second set: Transcript levels of *NMT1* and *METAP2* in PBMC isolated from whole blood sample using density gradient centrifugation (Ficoll), where Log 2 (fold change) expression values shown on y-axis are calculated relative to the *RPLP0*. Control (C), non-adenomatous polyps (P), adenomatous polyps (AP), and CRC patients are shown on x-axis. *METAP2* and *NMT1* was significantly lower in control patients. 17

Figure 9. Transcript levels of *NMT1* and *METAP2* in PBMC isolated from whole blood sample using density gradient centrifugation (Ficoll), where Log 2 (fold change) expression values shown on y-axis are calculated relative to the average *GAPDH* and *RPLP0*. Control, non-adenomatous polyps, adenomatous polyps, and CRC patients are shown on x-axis. *NMT1* and *METAP2* expressions was lowest in control patient however, *NMT1* and *METAP2* was the highest in patients with non-adenomatous polyp. *METAP2* was lower than *NMT1* in PBMC in CRC patients. 17

Figure 10. The PI3K/Akt/mTOR pathway plays an essential role in cell proliferation. 25

Figure 11. Rapamycin is a macrocyclic antibiotic that inhibits the highly conserved protein kinase target of rapamycin (TOR) by forming a complex with FKBP12, which then binds directly to mammalian TOR complex 1 (mTORC1) and inhibits mTOR pathway.	28
Figure 12. Rapamycin binds the intracellular receptor, interfering with growth-promoting cytokine signaling. This is done through inhibition of mTOR autophosphorylation and phosphorylation of initiation factor 4E binding protein, 4EBP1, which plays an important role in translation.	29
Figure 13. NMT1 protein expression by Western blot was assessed in WT ES and <i>Nmt1</i> ^{-/-} ES cells by different antibodies (Figure 13A). Relative normalized <i>Nmt1</i> gene expression was assessed by RT-PCR in <i>Nmt1</i> ^{+/-} ES, <i>Nmt1</i> ^{-/-} and WT ES cells (Figure 13B).	34
Figure 14. <i>Nmt1</i> ^{-/-} ES cells show increased PI3K p110 α expression. WT ES and <i>Nmt1</i> ^{-/-} ES cells were treated with rapamycin (10 nM) and/or insulin (100 nM) for 24 hrs. The cells were lysed and the lysates were assessed by Western blot for the expression of the catalytic subunit of PI3K, p110 α (Figure 14A). The right panel shows the corresponding densitometry (Figure 14B). The same membrane was stripped and re-probed with NMT1 (Figure 14C).	36
Figure 15. Akt and GSK phosphorylation was upregulated in <i>Nmt1</i> ^{-/-} ES cells upon insulin treatment. WT ES and <i>Nmt1</i> ^{-/-} ES cells were treated with rapamycin (10nM) and/or insulin (100nM) for 24 hrs. The cells were lysed and the lysates were assessed by western blot for the phosphorylation of Akt (Figure 15A) and GSK3 (Figure 15C). The same blots were stripped and re-probed with Abs against total Akt and GSK3 and used as loading controls. The right panel shows the corresponding densitometry (Figure 15B and 15D). The Western blot results represent one of three independent experiments with similar findings.	37

Figure 16. mTOR and IGF1R phosphorylation was upregulated in *Nmt1*^{-/-} ES cells compared to WT cells. WT ES and *Nmt1*^{-/-} ES cells were treated with rapamycin (10nM) and/or insulin (100nM) for 24 hrs. The cells were lysed and the lysates were assessed by Western blot for the phosphorylation of mTOR (Figure 16A) and IGF1R (Figure 16C). The same blots were stripped and re-probed with Abs against total mTOR and IGF1R and used as loading controls. The right panel shows the corresponding densitometry (Figure 16B and 16D). The Western blot results represent one of three independent experiments with similar findings. 39

Figure 17. AMPK phosphorylation was upregulated in WT ES cells compared to *Nmt1*^{-/-} ESC cells. 40

List of Appendices

Appendix A: To maintain ESC media 50

Appendix B: 0.05% Trypsin-EDTA (5mL) 51

Appendix C: PBS (10X) (1 Litre)	51
Appendix D: Lysis Buffer Preparation for Phosphoproteins (500 mL)	51
Appendix E: Micro BCA™ Protein Assay Kit Working Reagent	52
Appendix F: Loading Buffer (4X)	52
Appendix G: 30% Acrylamide (100 mL)	53
Appendix H: 1M TRIS (pH 6.8) (500 mL)	54
Appendix I: 1.5 TRIS (pH 8.8)	54
Appendix J: Running Buffer (10X) (2 Litres)	54
Appendix K: Transfer Buffer (5 Litres)	54
Appendix L: Blocking Solution (100 mL)	54
Appendix M: 1X PBS-T (1 Litre)	55
Appendix N: Protocol for mild stripping PVDF membranes Buffer, 1 liter	55
Appendix O: G418 (Geneticin)	55
Appendix P: Protein Estimation Protocol	56
Appendix Q: RNA Protocol	56
Appendix R: cDNA Synthesis kit	56
Appendix S: cDNA Thermocycler: Incubation Time	57
Appendix T: RT-PCR Primer Information	57
Appendix U: RT-PCR SYBR Green Mastermix	59
Appendix V: Whole Blood Study: Patient’s Colonoscopy/ Pathology Report	60
Appendix W: PBMC Study: Patients’ Colonoscopy/ Pathology Report	61

List of Abbreviations

Abbreviation	Name

Akt/PKB	Protein Kinase B
AMPK	Adenosine Monophosphate Kinase
AP	Adenomatous Polyp
ATP	Adenosine Triphosphate
APS	Ammonium Persulfate
BCA	Bicinchoninic Acid
BSA	Bovine Serum Albumin
CRC	Colorectal Cancer
cDNA	Complementary Deoxyribonucleic Acid
c-Src	Cellular-Src (sarcoma) Protein Kinase
DMEM	Dulbecco's Modified Eagle Medium
DMSO	Dimethyl Sulfoxide
DNA	Deoxyribonucleic Acid
DTT	Dithiothreitol
EDTA	Ethylenediaminetetraacetic Acid
EGTA	Egtazic Acid
FBS	Fetal Bovine Serum
G418	Geneticin (eukaryotic antibiotic)
GAPDH	Glyceraldehyde-3-Phosphate Dehydrogenas
GMEM	Glasgow Minimum Essential Medium
GNAT	GCN5-related N-acetyltransferase
GS	Glycogen Synthase
GSK 3 α/β	Glycogen Synthase Kinase-3 α/β

IGF	Insulin-like Growth Factor
IGF1R	Insulin-like Growth Factor Receptor 1
IR	Insulin Receptor
IRS1	Insulin Receptor Substrate 1
kDa	Kilo Dalton
KO	Knockout
LIF	Leukemia Inhibitory Factor
ME	2-Mercaptoethanol
METAP1	Methionine aminopeptidase 1
METAP2	Methionine aminopeptidase 2
mESC	Mouse embryonic stem cell
mRNA	Messenger ribonucleic acid
mTOR	Mechanistic Target of Rapamycin (Protein Kinase)
mTORC1	Mammalian Target of Rapamycin Complex (Raptor)
mTORC2	Mammalian Target of Rapamycin Complex (Rictor)
NMT1	N-myristoyltransferase 1
NMT2	N-myristoyltransferase 2
NME	N-terminal methionine excision
NAP	Non-adenomatous polyp
p70S6K	40S ribosomal protein S6 Kinase
P110 α	Catalytic subunit alpha
PBS	Phosphate Buffered Saline

PBST	Phosphate Buffered Saline with Tween 20 Detergent
PKB	Protein kinase B
PDK1	Phosphoinositide dependent protein kinase-1
PIC	Protease Inhibitor Cocktail
PI3K	Phosphatidylinositide 3-kinase
PIP2	Phosphatidylinositol-4,5-bisphosphate
PIP3	Phosphatidylinositol-3,4,5-trisphosphate
PMSF	Phenylmethylsulfonyl Fluoride
PTEN	Phosphatase and Tensin Homolog
PVDF	Polyvinylidene Difluoride
qRT-PCR	Quantitative Real-Time Polymerase Chain Reaction
RNA	Ribonucleic Acid
RO	Reverse Osmosis
RPLP0	Ribosomal Protein Lateral Stalk Subunit P0
RTK	Receptor Tyrosine Kinase
SDS	Sodium Dodecyl Sulfate
SDS-PAGE	Sodium Dodecyl Sulfate Polyacrylamide Gel Electrophoresis
SH2	Src Homology 2
TEMED	Tetramethylethylenediamine
WT	Wild Type

CHAPTER 1: N-myristoyltransferase 1 and Methionine Aminopeptidase 2 are novel biomarkers for early detection of colorectal adenomatous polyps and cancers

Colorectal Cancer

Colorectal cancer (CRC) is a common malignant disease and a major cause of mortality worldwide. Currently, it is the second most commonly diagnosed cancer in Canada, affecting approximately 25,000 Canadians [1]. CRC accounts for 13% of the annual incidence of cancer in Canada for men and 11% for women [1]. According to American Cancer Society, 1 in 22 men and 1 in 24 women are at a risk of developing the disease. The estimated number of CRC cases in United States for 2017 were reported to be as high as 95, 270 new cases of colon cancer and 39, 220 new cases of rectal cancer [2]. Compared to other cancers, CRC is a highly treatable cancer if it is detected early and it is up to 90% preventable with timely and thorough CRC screening. Unfortunately, as it stands today, nearly half of those diagnosed find out too late [2]. There are two types of colon polyps: non-neoplastic polyps and neoplastic polyps [3]. The non-neoplastic polyps are hyperplastic or inflammatory (non-adenomatous) but are non-precancerous. However, neoplastic polyps (adenomatous polyps or adenomas), are benign neoplasms that can progress to form cancer and are precancerous in nature (Figure 1) [3]. Adenomatous polyps display some dysplasia, which can be graded into mild, moderate, and severe based on histology. Neoplastic polyps are histologically divided into 3 sub-groups: tubular adenomas, villous adenoma and mixed. Patients with tubular adenomas are at a 3% risk of malignant tumor formation; while villous adenomas have 15% or higher risk of malignant formation [4, 5]. Due to their malignant nature, these polyps should be

identified and removed at the early stage to avoid the development of CRC. CRC begins as adenomatous polyps which is benign growth in the lining of the colon. Over the years, these adenomatous polyps grow larger and can differentiate, thereby increasing the risk of cells in the polyps becoming cancerous. Therefore, early detection of adenomatous polyps is an important step in preventing progression of CRC. It is important to identify and remove these polyps as soon as possible. Since CRC develops slowly from precancerous lesions, early detection and prompt removal of adenoma can decrease the incidence and mortality rate. Once polyps are detected, especially adenomatous polyps, an increased risk for colorectal carcinoma must be anticipated and appropriate surveillance becomes mandatory even after polypectomy. If the adenomatous polyps are not treated or removed they can develop into cancers, a process that takes at least 10 years [6]. Early detection is the key to survival, however the surgical resection of the growth, often in combination with chemotherapy, significantly increases life expectancy. Currently available CRC screening tests such as fecal occult blood testing (FOBT), sigmoidoscopy, and colonoscopy have several limitations including: limited efficacy, the invasive nature of the test, and poor patient compliance [7].

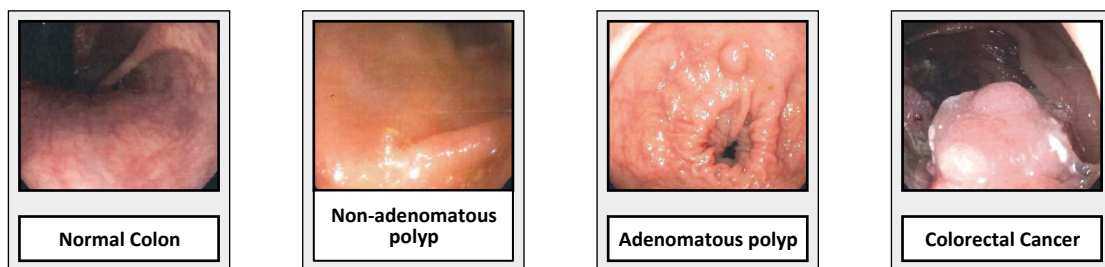


Figure 1. Photographs showing normal, non-adenomatous polyp (NAP), adenomatous polyp (AP), and CRC colon.

N-myristoyltransferase (NMT) and Myristoylation

Acylation of proteins by long chain fatty acids promotes binding of proteins to the inner leaflet of the plasma membrane and regulates their intracellular trafficking [8]. N-myristoylation is an irreversible modification and co-translational lipid modification that involves the covalent attachment of a 14-carbon saturated myristoyl group to the N-terminal glycine residue of a target protein. The myristoyl transfer is catalyzed by N-myristoyltransferase (NMT) (Figure 2), and is known to occur in viruses, fungi, plants and in mammals, including mice, rats and humans. [9-13]. A myriad of proteins involved in a variety of signaling cascades and cellular differentiation are myristoylated [10, 11]. These include the catalytic subunit of cAMP-dependent protein kinase [14], the β -subunit of calcineurin [15], the α -subunit of several G-proteins [16], non-receptor tyrosine kinases such as Lck of T cells and the cellular and transforming forms of pp60src [17]. The eukaryotic NMT is a member of the GCN5-related N-acetyltransferase (GNAT) superfamily of proteins [9-11].

NMT and METAP2

Lipid modification of proteins has received great attention recently as a target for therapeutic interventions to cancer [18]. Myristoylated proteins are involved in a variety of signal transductions, cellular proliferation, and oncogenesis [18]. Myristoylation is an integral part of apoptosis or programmed cell death [18]. In the PI3K/Akt/mTOR pathway, c-Src is frequently observed to be activated or over-expressed in a number of human cancers; especially those of colon and breast. Activation of c-Src and its subsequent oncogenic growth signaling requires myristoylation. In 1995, it was first

discovered that there was an increase in NMT enzyme activity in rat colonic cancer tissue compared to adjacent normal-appearing cells. To confirm that this phenomenon was not specific to the rat model, a small sample of human colonic adenocarcinomas tissue were measured to have hyperactivity of NMT [19]. In mammalian systems, NMT activity has been shown to increase in colorectal tumors, leading to the proposal that NMT enzyme could serve as a target for anticancer therapies [20] and the possibility of NMT having a vital role in human tumor progression. After 2 years, the same group correlated NMT Enzyme activity to NMT protein expression by using Western blot analysis. The results showed that all the human colonic tumor samples had high NMT protein expression.

A newly synthesized protein will always have a methionine group at the N-terminal. Methionine aminopeptidase (MetAP2) cleaves the Methionine residue and removes it. The end product is an N-terminus glycine residue protein. An N-terminus glycine residue protein is the only protein that can be myristoylated. Thus, MetAP2 is an upstream event and it is an important part of myristoylation reaction. In order for NMT to catalyze myristoylation at the N-terminal glycine of a target protein, the removal of N-terminal methionine is required, as it is essential for further amino-terminal modifications and the maturation of many proteins. The methionine aminopeptidases (MetAPs) represent a unique class of proteases which remove the initiation methionine residue from newly synthesized polypeptide chains [21]. MetAPs catalyze N-terminal methionine excision (NME) - an essential pathway of co-translational protein maturation (Figure 2) [22]. In some instances, the action of MetAP is required for biological activity, proper subcellular localization, and eventual degradation. This enzyme is present in both

eukaryotes and prokaryotes [22]. In yeast and humans, two proteins are known to possess MetAP activity: MetAP1 and MetAP2. MetAP2 has attracted much more attention than MetAP1 due to its discovery as a target molecule of the anti-angiogenic compounds fumagillin and ovalicin. In 2006, reports from Western blot analysis shows a higher expression of MetAP2 in all cases of cancerous tissues compared with normal tissues. In addition, immunohistochemistry analysis revealed that all cases of colorectal adenocarcinoma show strong cytoplasmic positivity for MetAP2 with increased intensity in the invasive component [23]. In summary, both NMT and MetAP2 were over-expressed in the colonic tumor. In 2007, Dr. Shrivastav's group investigated whether those molecular signatures can be found in peripheral blood, as blood is easier to collect and it is an alternative to tissue samples. They found an over-expression of NMT1 in peripheral blood smears of rats with cancer relative to healthy rats [24]. In addition, they collected blood samples from patients with cancer and they found an over-expression of NMT1 in peripheral blood smears in cancer patients compared to healthy individuals [24]. Overall, there was a high expression of NMT in both colonic tumors and peripheral blood samples, but there have only been reports on the high expression of MetAP2 in the colonic tumor.

Since the myristoylation reaction is catalyzed by NMT, after removal of methionine by MetAP2, I investigated the correlation between MetAP2 and NMT1. It appears that higher expression of MetAP2 is required for the over-expression of NMT1 in colon carcinogenesis. The elevated NMT activity during colonic carcinogenesis may be due to the higher demand for myristoylation of various proteins/oncoproteins which are

overexpressed and activated during tumorigenesis. A direct relationship between elevated NMT expression and activity in colon cancer progression has been reported [18]. NMT1 and MetAP2 can be a putative therapeutic drug target for CRC if the patient is diagnosed at an early stage. This study focused on the role of NMT1 and METAP2 gene expression in healthy, noncancerous adenomatous polyps, and CRC patients. These enzymes can be modulated by growth factors [25] and may be of importance in cancer development and therapy.

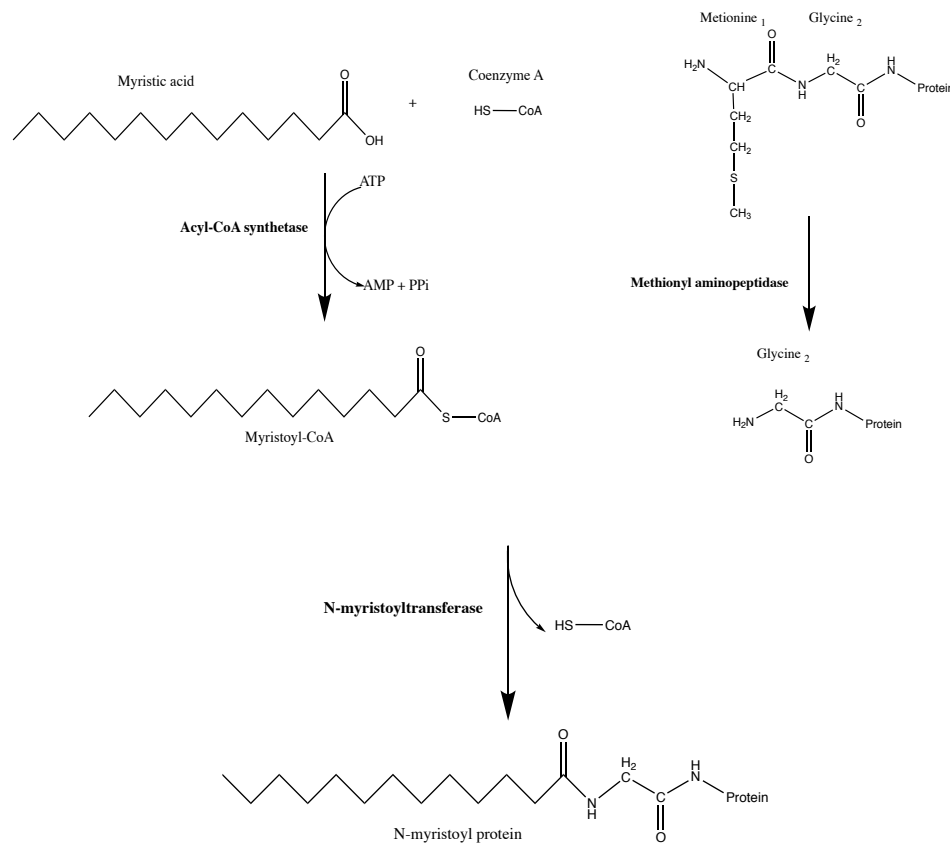


Figure 2. Myristoylation reaction catalyzed by N-myristoyltransferase (NMT). The myristoyl functional group is added to the N-terminal glycine residue co-translationally following the removal of the N-terminal methionine residue by methionine aminopeptidase (MetAP) and the synthesis of myristoyl-CoA by acyl-CoA synthetase.

Whole Blood

The peripheral blood expression profile represents a promising tool to discover biomarkers associated with physiological or pathological events. Circulating blood is easily accessible and can represent an alternative to tissue sampling for the purpose of finding molecular signatures. Here in we describe measuring gene expression from patient whole blood samples. This method consists in the combination of PAXgene™ tubes containing an mRNA stabilizer for blood collection, and the PAXgene Blood RNA Kit (IVD) for nucleic acid purification. The PAXgene Blood RNA System is intended for the isolation and purification of intracellular RNA for RT-PCR used in diagnostic testing.

Peripheral Blood Mononuclear Cell (PBMC)

The isolation of peripheral blood mononuclear cells (PBMC) from whole blood allows for the purification of immune system associated cells (Figure 3) [26]. These cells are able to respond to internal and external signals, and therefore have been proposed as a source of biomarkers of conditions and diseases, as their gene expression profile may reflect the physiological and pathological state of the organism. PBMCs are mainly comprised of monocytes, macrophages, T cells, B cells, natural killer (NK) cells, and dendritic cells (Figure 3). Thus, PBMCs contain different cell types that play important roles in the immune system such as monitoring immune-relevant events and response to inflammation [27]. The use of state-of-the-art proteomic profiling methods in PBMCs will enable minimally invasive monitoring of disease progression or response to treatment and discovery of biomarkers [27].

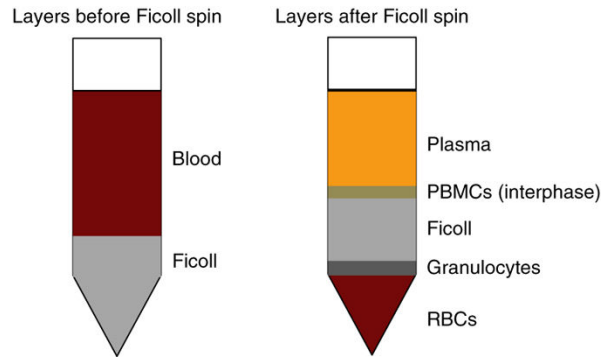


Figure 3. Isolation of PBMC by Ficoll-Paque density gradient centrifugation: The bottom layer is made up of red blood cells (erythrocytes) collected or aggregated by the Ficoll medium and sink completely through to the bottom. The next layer up from the bottom is primarily granulocytes, which also migrate down through the Ficoll-Paque solution. The next layer towards the top is the PBMC, which are typically at the interface between the plasma and the Ficoll solution, along with monocytes and platelets. To recover the PBMC, this layer is carefully recovered, washed with a HBSS to remove platelets, Ficoll, and plasma, then centrifuged again.

HYPOTHESIS

“*NMT1* and *METAP2* RNA transcripts are overexpressed in colorectal cancer patients’ peripheral blood mononuclear cells and whole blood samples and may translate into an effective biomarker for early detection of the disease and could possibly translate into a blood-based test for CRC screening.”

OBJECTIVE

The aim of the study is to investigate the patterns of gene expression of *NMT1* and *METAP2* in healthy control, non-adenomatous polyps, adenomatous polyps, and CRC patients’ whole blood and PBMC via the RT-PCR technique.

MATERIALS AND METHODS

Whole blood study: RNA isolation with PAXgene® kit

Blood samples from 18 participants including: 3 controls, 4 non-adenoma polyps, 4 adenoma polyps, and 7 CRC patients were collected over the course of 1 year from September 2014 to April 2015. All participants went for colonoscopy at the Health Sciences Center (Winnipeg, Manitoba) and provided signed informed consent prior to their blood samples being obtained by venipuncture for accurate quantification of peripheral blood mRNA levels. A 2.5 ml sample of blood was transferred to a PAXgene™ tube for immediate cell lysis and nucleic acid precipitation. The mRNA is stable for up to 5 days in the blood lysate, provided the tubes are kept at room temperature until mRNA extraction. The PAXgene blood RNA kit (PreAnalytiX) was used for RNA extraction, according to the manufacturer's protocol.

PBMC study: RNA isolation using Ficoll-Hypaque gradient centrifugation

Blood samples from 25 participants containing: 9 controls, 7 non-adenoma polyps, 6 adenoma polyps, and 3 CRC patients were collected from August 2017 to February 2018. All participants went for colonoscopy at the Health Sciences Center (Winnipeg, Manitoba) and provided signed informed consent prior to their blood samples being obtained by venipuncture for accurate quantification of peripheral blood mRNA levels. Blood samples were collected in EDTA tubes and PBMCs were isolated by Ficoll-Hypaque gradient centrifugation. A Total RNA Kit was used for RNA extraction from PBMC (Omega Bio-Tek) according to the manufacturer's protocol.

RNA Quantification

The concentration and the purity of total RNA was measured using the ratio of absorbance at 260nm and 280nm (A_{260}/A_{280}) with a SpectraMax^R i3 spectrophotometer, and SoftMax software. The SpectraDrop Micro-Volume Microplate can confirm that the sample is free of protein (A_{260}/A_{280}) if the ratio ranges between 1.8 to 2.0.

cDNA Synthesis: Reverse Transcription of mRNA

RNA samples were prepared for as follows: Total RNA (1 μ g) was reverse-transcribed using the iScript Reverse Transcription Supermix for RT-PCR (Bio-Rad) in a total volume of 20 μ l according to the manufacturer's instructions; The reaction mixture was incubated at 25 °C for 5 min for priming, then at 42 °C for 60 min for reverse transcription, and finally at 85 °C for 5 min for reverse transcriptase inactivation. The complementary DNA (cDNA) was stored at -20 °C until further use.

Primers

Quantitative PCR was performed on two target genes: *NMT1* and *METAP2*; and three housekeeping genes: *GAPDH*, *ACTB*, and *RPLP0*. Information for all primers used is listed in Appendix T.

Real Time Quantitative RT-PCR Analysis

The expression of *NMT1* and *METAP2* was measured using RT-PCR. For amplification and data collection I used the CRX ConnectTM Real-Time System Cycler and CFX Manager 3.1 software (BioRad). The optimal reaction conditions were obtained

with 1x SsoAdvanced™ Universal SYBR® Green Supermix, 300 nM specific primer, RNase/DNase-free water, and cDNA template (20 ng/well) up to final volume of 15 µl/well. Amplifications were performed starting with a 30 sec enzyme activation cycle at 95 °C, followed by 40 cycles of denaturation at 95 °C for 5 sec, 1 cycle of annealing/extension at 60 °C for 30 sec, and a final cycle at 72 °C for 30 sec. At the end of each run a melting curve analysis was done from 65 °C to 95 °C for 0.5 to 5 sec. All samples were amplified in triplicates, and the obtained cycle of quantification (Cq) value was then used for further analysis. Cq values of >35 were excluded from further mathematical calculations. A NTC “no template sample” (RNA from reverse transcription without reverse transcriptase) and a sample without RNA or cDNA were the negative controls.

Calculation of the amounts of gene expression

The relative gene expression was calculated by the subtraction of the Cq value of *NMT1* (target gene) in the samples relative to *GAPDH* and *ACTB* (housekeeping gene) for whole blood samples. *GAPDH* and *RPLP0* was the housekeeping gene for PBMC samples. Relative quantification is the most commonly used method [28].

Step 1. Normalize to (REF): $\Delta Cq = Cq (\text{Target gene}) - Cq (\text{Housekeeping genes})$

Step 2. Exponential expression transform: $\Delta Cq \text{ Expression} = 2^{(-\Delta Cq)}$

RESULTS

1. *NMT1* and *METAP2* gene expression in Whole Blood

Expression was measured by RT-PCR to examine the relative transcript levels of *NMT1* and *METAP2* in 18 patients, which consisted of healthy controls (n=3), non-adenomatous polyps (n=4), adenomatous polyps (n=4), and CRC patient (n=7) whole blood samples (Figure 4 & 5). Analysis of the real-time RT-PCR results was performed by a relative quantification method whereby the change in expression of the target gene: *NMT1* and *METAP2* is determined relative to the average expression of *GAPDH* and *ACTB* housekeeping genes.

Both *NMT1* and *METAP2* were detected in all the individuals (Figure 4 & 5). The overall expression of *NMT1* and *METAP2* was seen to be the highest in the non-adenomas polyp samples with *METAP2* being consistently higher than *NMT1* (Figure 6). *METAP2* and *NMT1* expression patterns showed no significant differences in patient healthy control and non-adenomatous polyp samples. However, expression was the lowest in the healthy control compared to non-adenomatous polyps, adenomatous polyps and CRC (Figure 6). *METAP2* expression was the lowest in the adenomatous polyp but increased by over 0.08-fold in control, 0.60-fold non-adenomatous polyps and 0.64-fold CRC patients (Figure 6). There was a significant increase in *METAP2* in CRC whole blood samples. *NMT1* showed a similar trend, expression was the lowest in the adenomatous polyp but increased by over 0.07-fold in control, 0.30-fold CRC and 0.58-fold non-adenomatous polyp patients (Figure 6). There was a significant increase in *METAP2* than *NMT1* in CRC whole blood samples.

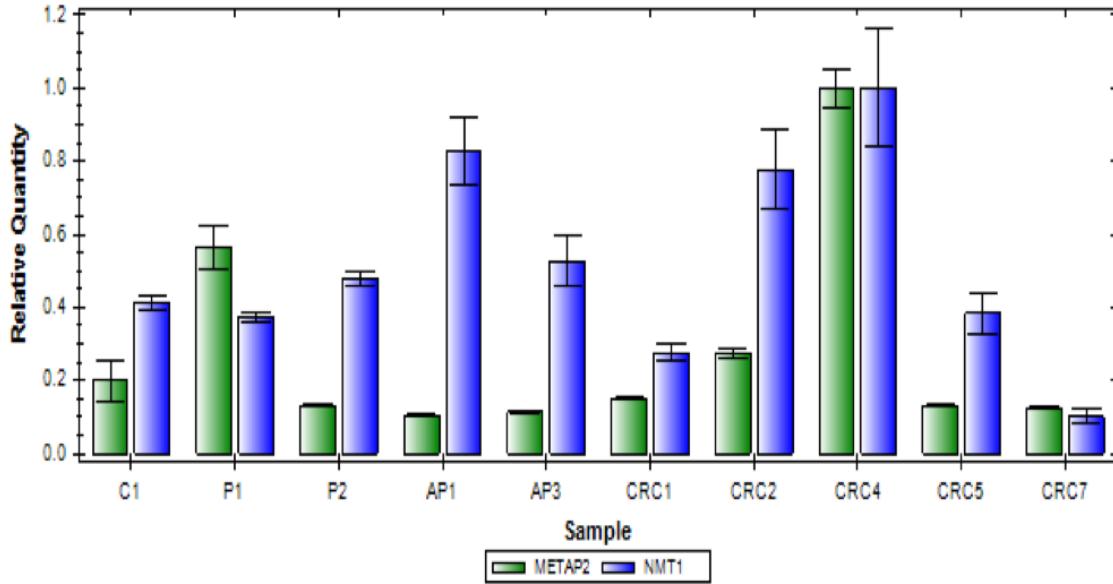


Figure 4. First set: Transcript levels of *NMT1* and *METAP2* from whole blood (PAXgene Tube), where Log₂ (Fold change) expression values shown on y-axis are calculated relative to *GAPDH* and *ACTB*. Control (C), non-adenomatous polyps (P), adenomatous polyps (AP), and CRC patients are shown on x-axis.

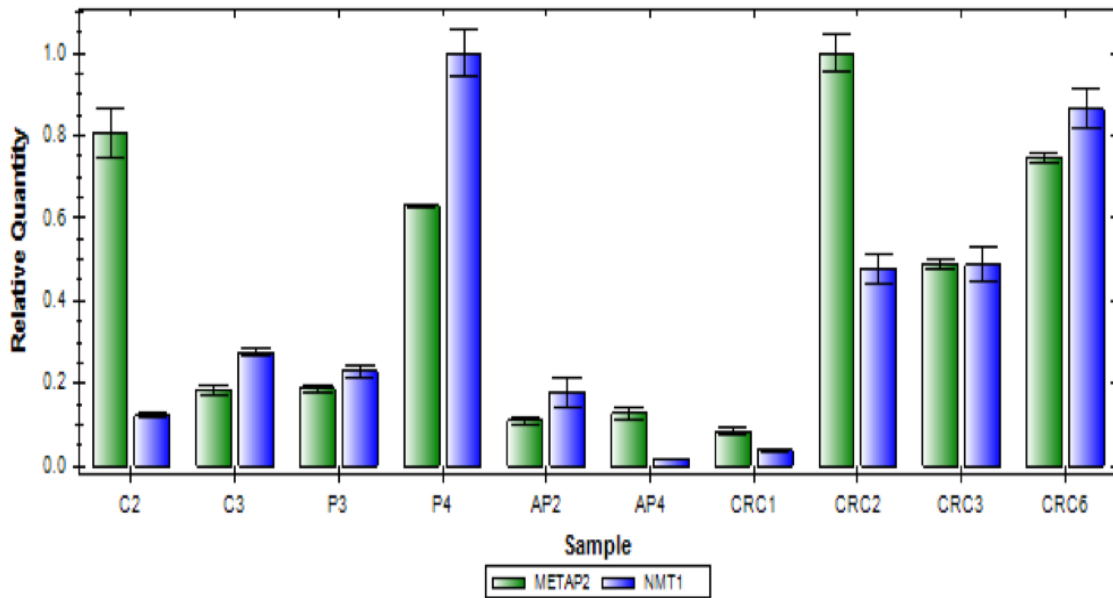


Figure 5. Second set: Transcript levels of *NMT1* and *METAP2* from whole blood (PAXgene Tube), where Log₂ (Fold change) expression values shown on y-axis are calculated relative to *ACTB*. Control (C), non-adenomatous polyps (P), adenomatous polyps (AP), and CRC patients are shown on x-axis.

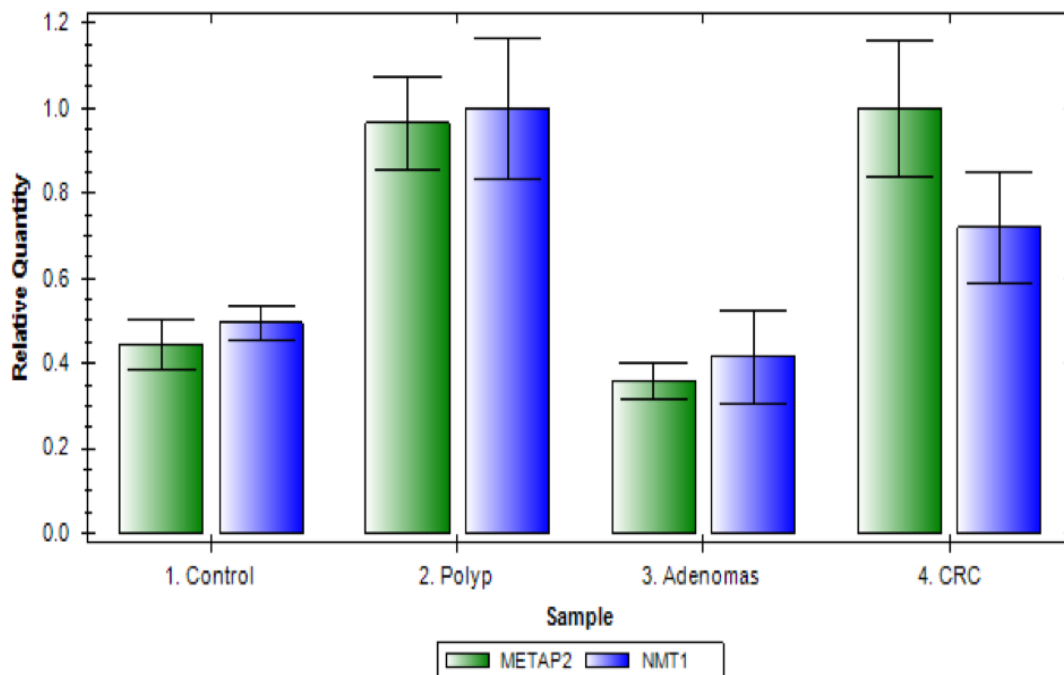


Figure 6. Transcript levels of *NMT1* and *METAP2* from whole blood (PAXgene Tube), where Log₂ (Fold change) expression values shown on y-axis are calculated by relative to the average housekeeping genes: *GAPDH* and *ACTB*. Control, non-adenomatous polyps, adenomatous polyps, and CRC patients are shown on x-axis. *NMT1* and *METAP2* expression was lowest in adenomatous patients; however, *NMT1* and *METAP2* was the highest in non-adenomatous polyp and CRC patients. *METAP2* was significantly higher than *NMT1* in CRC patients' whole blood sample.

2. *NMT1* and *METAP2* gene expression in PBMC

Expression was measured by RT-PCR to examine the gene expression of *NMT1* and *METAP2* in PBMC samples from 25 patients, which consisted of healthy controls (n=9), non-adenomatous polyps (n=7), adenomatous polyps (n=6), and CRC patients (n=3) (Figure 7 & 8). Analysis of the real-time RT-PCR results was performed by a relative quantification method whereby the change in expression of the target gene: *NMT1* and *METAP2* is determined relative to the *GAPDH* and *RPLP0* housekeeping genes.

The overall expression of *NMT1* and *METAP2* was higher in the non-adenomatous polyps, adenomatous polyps, and CRC compared to healthy control samples (Figure 9). *METAP2* expression was lowest in the healthy controls but increased by over 0.16-fold in CRC, 0.25-fold adenomatous polyps and 0.96-fold non-adenomatous patients (Figure 9). There was a significant increase in *METAP2* in CRC whole blood samples. *NMT1* showed a similar trend, expression was the lowest in the healthy controls but increased by over 0.34-fold in CRC, 0.30-fold adenomatous polyps and 0.95-fold non-adenomatous patients (Figure 9). There was a significant increase in *NMT1* in CRC PBMC samples.

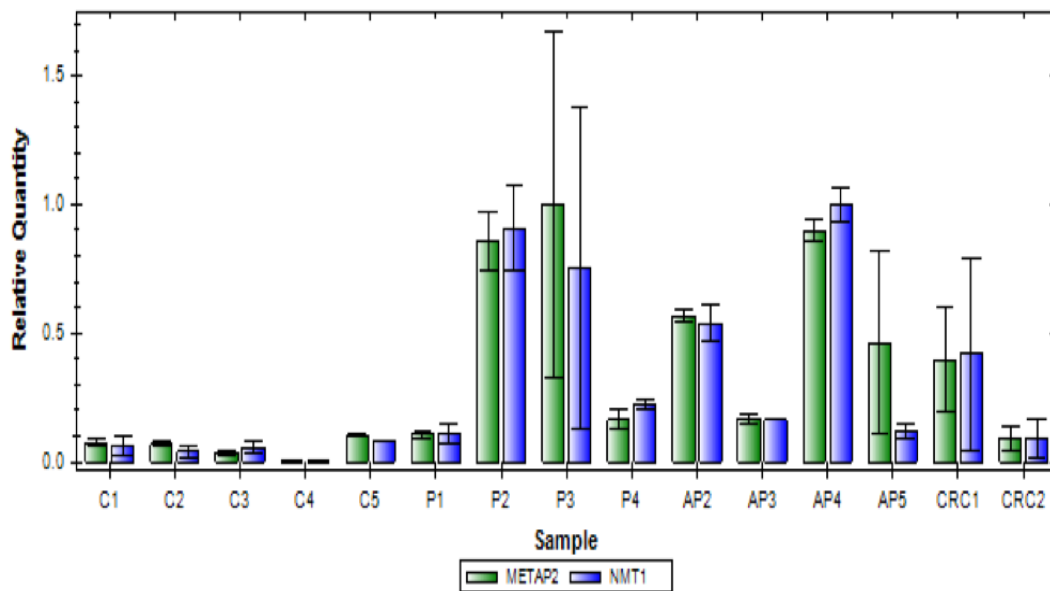


Figure 7. First set: Transcript levels of *NMT1* and *METAP2* in PBMC isolated from whole blood sample using density gradient centrifugation (Ficoll), where Log₂ (fold change) expression values shown on y-axis are calculated relative to the *GAPDH*. Control (C), non-adenomatous polyps (P), adenomatous polyps (AP), and CRC patients are shown on x-axis. *METAP2* and *NMT1* was significantly lower in control patients.

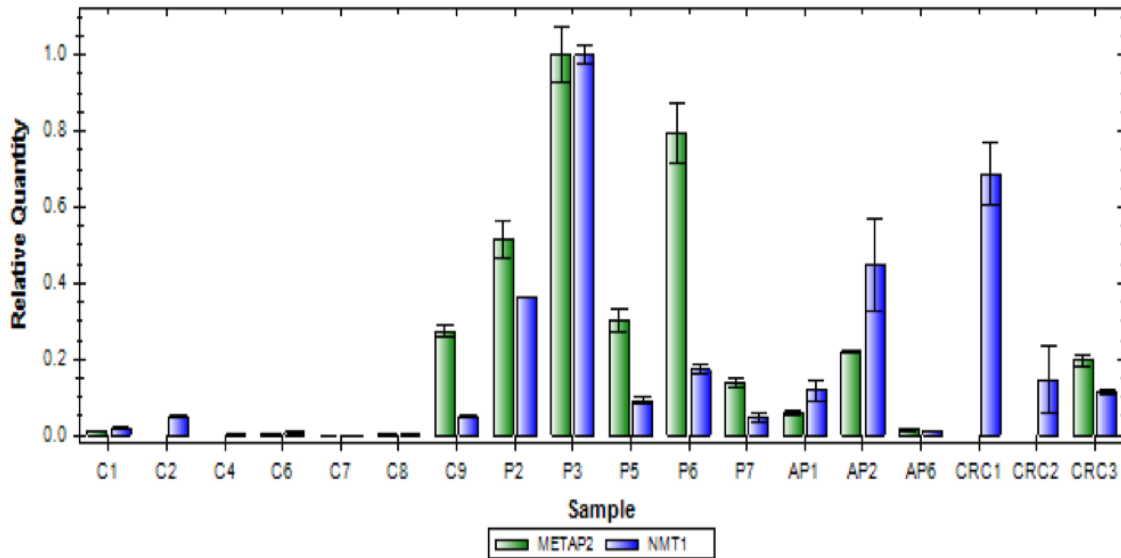


Figure 8. Second set: Transcript levels of *NMT1* and *METAP2* in PBMC isolated from whole blood sample using density gradient centrifugation (Ficoll), where Log₂ (fold change) expression values shown on y-axis are calculated relative to the *RPLP0*. Control (C), non-adenomatous polyps (P), adenomatous polyps (AP), and CRC patients are shown on x-axis. *METAP2* and *NMT1* was significantly lower in control patients.

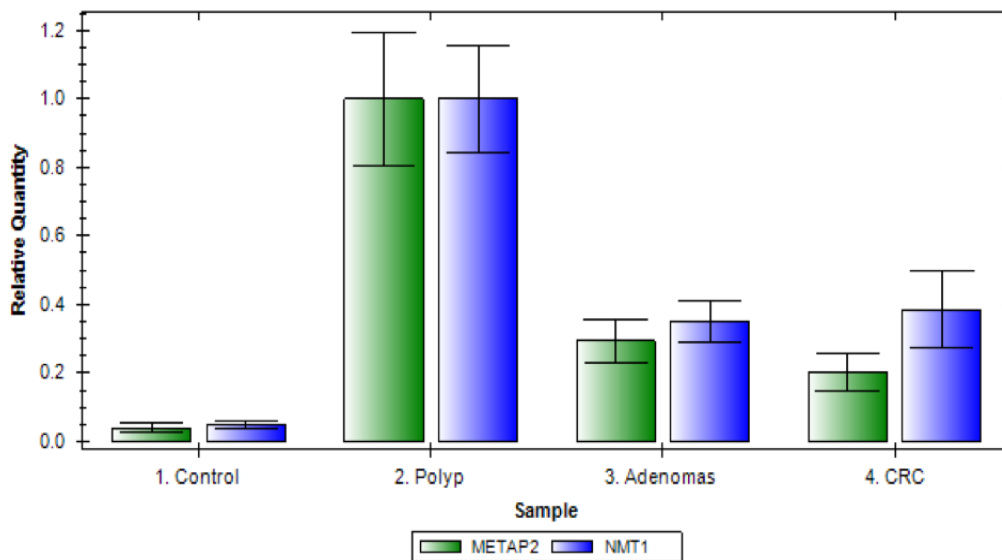


Figure 9. Transcript levels of *NMT1* and *METAP2* in PBMC isolated from whole blood sample using density gradient centrifugation (Ficoll), where Log₂ (fold change) expression values shown on y-axis are calculated relative to the average *GAPDH* and *RPLP0*. Control, non-adenomatous polyps, adenomatous polyps, and CRC patients are shown on x-axis. *NMT1* and *METAP2* expressions was lowest in control patient however, *NMT1* and *METAP2* was the highest in patients with non-adenomatous polyp. *METAP2* was lower than *NMT1* in PBMC in CRC patients.

DISCUSSION

N-myristoylation is a lipid modification found in mammalian, fungal, plant, and viral proteins. The enzyme mediating the protein myristoylation, N-myristoyltransferase (NMT), covalently attaches a 14-carbon fatty acyl group (myristoyl group) to a glycine residue at the N-terminus of a protein. The known myristoylated proteins include the catalytic subunit of cAMP-dependent protein kinase, various tyrosine kinases (pp60^{c-src}), the β -subunit of calmodulin-dependent protein phosphatase (calcineurin), the myristoylated alanine-rich C-kinase substrate, and the α -subunit of several G proteins [23]. The myristoylated protein has multiple functions such as membrane localization, protein translocation, and oncogenesis.

In general, protein myristoylation is a co-translational process that occurs after the removal of methionine by methionine aminopeptidase (MetAP). Methionine aminopeptidase 2 (MetAP2) is a bifunctional protein that plays a critical role in the regulation of post-translational processing and protein synthesis. The main aim of this study was to investigate the gene expression of *NMT1* And *METAP2* in whole blood and PBMC in HSC patients by Real Time RT-PCR methods. RT-PCR was chosen because it is highly specific, sensitive, and can detect the gene expression of multiple genes at one time. Moreover, it is one of the most reliable methods of quantifying mRNA and is therefore well-suited to the application of helping to triage patients who are waitlisted for colonoscopy and is a favorable option for the analysis of cancer markers [29].

I quantitatively evaluated the expression profile of 2 target genes: *NMT1* and *METAP2* in both whole blood and PBMC from healthy controls, non-adenomatous polyps, adenomatous polyps, and CRC patients. Here we show that both *NMT1* and *METAP2* were overexpressed in PBMCs from the CRC patients. This result demonstrated that both the enzymes NMT and MetAP play a major role in the process of myristoylation of oncoproteins, and more glycine terminal protein is required by the cells for proliferation and cancer development. When both genes were compared, *METAP2* expression was found to be higher than *NMT1* and it was significantly more prevalent in CRC. The high expression of *METAP2* in human colorectal carcinoma, revealed the potential role of MetAP2 in cancer. The high level of *METAP2* activity in colon cancer correlates with both an increase in enzyme synthesis and an association of the activated kinase with the cytoskeleton. MetAP2 is also known as the molecular target of the angiogenesis inhibitor TNP-470 [30]. There been reports that a high level of MetAP2 expression was observed in B cells of malignant lymphomas [31].

All the samples had similar gene expression except in adenomatous polyps from the whole blood and PBMC. In whole blood, *NMT1* gene expressed higher than *METAP2*, but in PBMCs the *NMT1* expressed lower than *METAP2*. The discrepancy in expression profile of *NMT1* and *METAP2* in whole blood and PBMC suggest that cells other than PBMC such as neutrophils have different pattern of expression for these genes. In an earlier study by Shrivastav et al have shown that neutrophil upon activation display differential expression of NMT1 compared to resting neutrophils.

Real-time PCR approaches are now widely applied in clinical research to quantify the abundance and expression of functional gene markers in biological samples. However, RT-PCR has significant limitations. Traditionally, false-positives due to carryover contamination have caused considerable problems in the routine implementation of qPCR in research and have led to strict guidelines in the design of laboratories dedicated to performing PCR. RT-PCR workflow has multiple steps, and there can be several sources of bias in gene measurement by RT-PCR that can alter the results. In the initial step, RNA extraction, excess use of 95% ethanol can crosslink RNA, and the presence of polysaccharides can reduce the elution of RNA. During the second step, in which the RNA is converted to cDNA, the presence of reverse transcriptase inhibitors can result in the incomplete conversion of all the RNA present into cDNA. The presence of inhibitors can significantly increase the measurement biases, and produce false negative or false positive results in both RT-PCR and cDNA reverse transcription.

An alternative to PCR is western blot analysis - a technique in which the activation of proteins in signaling pathways can be detected. Western blots can be used to study the protein expression of NMT1 and MetAP2. This method is sensitive and specific, and inexpensive compared to PCR. Another alternative to qPCR is immunofluorescence. Used observe the expression and localization on NMT1 and MetAP2 in PBMCs, this method is both quicker and inexpensive relative to PCR and Western blots Analysis.

Overall, RT-PCR is an excellent tool that may assist in the understanding of the molecular events underlying human cancer. An accurate RT-PCR analysis could improve clinical diagnosis as well as predictive and prognostic monitoring of disease. Furthermore, RT-PCR may offer tools to detect and measure gene expression at an early stage. The results demonstrate that when a patient's blood is over-expressing NMT1 or METAP2, they should be prioritized and screened for colorectal cancer. Screening can prevent colorectal cancer by finding and removing polyps before they turn into cancer. Early detection will result in a greater number of treatment options and better outcomes.

CHAPTER 2:

Functional Relevance of N-myristoyltransferase 1 in Cellular Growth Pathway

Mouse Embryonic Stem Cells

Mouse embryonic stem cells (mESC) are self-renewing, pluripotent cells derived from the inner cell mass of blastocyst stage mouse embryos. mESC, spontaneously differentiate into numerous cell types derived from all three embryonic germ layers [32]. Stem cells can be classified into three broad categories, based on their ability to differentiate. Totipotent stem cells are found only in early embryos. Each cell can form a complete organism (e.g., identical twins). Pluripotent stem cells exist in the undifferentiated inner cell mass of the blastocyst and can form any of the over 200 different cell types found in the body [33]. Multipotent stem cells are derived from fetal tissue, cord blood and adult stem cells [32]. Although their ability to differentiate is more limited than pluripotent stem cells, they already have a track record of success in cell-based therapies.

NMT and ESC

As is known, the N-myristoylation process is catalyzed by the enzyme N-myristoyltransferase. N-Myristoylated proteins comprise a large family of functionally diverse eukaryotic and viral proteins. Proteins that are destined to be covalently modified with the 14-carbon saturated fatty acyl group (myristoyl group) generally contain the sequence Gly-X-X-X-Ser/Thr at the amino terminus (Figure 2). The significance of NMT in normal cellular functioning is evident from a study where *Drosophila* embryos

with null NMT mutations displayed a range of abnormal phenotypes, including failure of head involution, dorsal closure, and germ-band retraction, all of which are strikingly similar to phenotypes caused by mutations to genes involved in dynamic rearrangement of the actin cytoskeleton. As just stated above, together with the recent demonstrations that showcase that the myristoylated non-receptor tyrosine kinases, Dsrc42A and Dsrc64B, are key regulators of cytoskeletal dynamics [34, 35], support the idea that myristoylated proteins have important functions in fundamental morphogenetic processes in *Drosophila* [36]. NMT in lower eukaryotes is encoded by a single NMT gene, whereas in higher eukaryotes such as bovines, humans, and plants, NMT is encoded by two NMT genes located on separate chromosomes. The second genetically distinct NMT cDNA (*NMT2*) has been cloned from a human liver library [37].

Since, NMT1 and METAP2 were found to be overexpressed in whole blood and PBMC of individuals with polyps and CRC, I wanted to further investigate the role of NMT1 in signaling proteins especially those of metabolic pathway which are known to be perturbed in CRC [38]. Furthermore, previous findings from our group suggest NMT1 is crucial for mouse embryo development and myelopoiesis. By knocking out the *Nmt1* gene in mice, it was demonstrated that NMT1 is the principal enzyme in early embryogenesis. Inter-crosses of *Nmt1*^{+/-} mice yielded no viable homozygotes (*Nmt1*^{-/-}). Since *Nmt1*^{-/-} Embryonic Stem cells (ES *Nmt1*^{-/-} KO) could be isolated, NMT1 does not appear to be essential for viability of mammalian cells, but it is required for the early embryonic development. Although both NMT isoforms share 77% amino acid sequence homology, they differ in substrate affinity [39]. NMT1 has been acknowledged to be the

principal isoform responsible during early embryogenesis of mice [40]. It has also been reported that NMT1 and regulated total NMT activity is essential for proper monocytic differentiation [41] and, using bovine neutrophils, it was demonstrated that NMT1 has a role in regulating neutrophil lifespan [42].

As demonstrated in the chapter 1, *NMT1* and *METAP2* genes were overexpressed in peripheral blood or PBMC of individuals with polyps and CRC. Based on previous reports where NMT1 has been demonstrated to be the downstream target of Akt [43], I was interested in investigating the effect of NMT1 knockout on PI3K/Akt/mTOR signaling pathway.

PI3K/Akt/mTOR Signaling Pathway

The PI3K/Akt/mTOR pathway is an important intracellular downstream pathway that regulates cellular growth, cell proliferation over differentiation (stem cells/ neural stem cells), protein synthesis, and apoptosis (Figure 2) [44]. Once this pathway is activated, it can propagate to downstream substrates including: receptor tyrosine kinases (RTK), PI3K, Akt/PKB, mammalian target of rapamycin (mTOR), and NMT. When this pathway is overactive, it can increase cell proliferation and inhibit apoptosis [45]. In order to activate this pathway, insulin or insulin-like growth factors must bind to the insulin-like growth factor-1 receptor (IGF-1R), which is a receptor tyrosine kinase (RTK). RTKs are composed of 2 extracellular alpha-subunits and 2 transmembrane beta subunits. This pathway is first initiated by insulin binding to the alpha-subunits of the RTK [46], [47]. Insulin binding causes autophosphorylation of the RTK beta subunits

that transduces downstream regulators and triggers phosphorylation of multiple substrates. Insulin receptor substrate 1 (IRS-1) is the first intracellular substrate of the RTK following autophosphorylation [45, 48]. This results in the activation of IRS-1 docking proteins, followed by PI3K. PI3K is composed of two subunits; one subunit houses two SH2 domains and another serves as a catalytic domain [49]. The PI3K substrate becomes activated by phosphorylation at the SH2 domain [49]. The activated protein approaches phosphatidylinositol-4,5,-bisphosphate (PIP₂), converting this phospholipid to phosphatidylinositol-3,4,5,-trisphosphate (PIP₃). The activation of Akt/PKB is facilitated by its binding to PIP₃, which in turn exposes the residues Ser⁴⁷³ and Thr³⁰⁸ [45, 48]. To fully activate Akt, phosphoinositide-dependent kinase 1 (PDK-1) phosphorylates Akt at Thr³⁰⁸ and mTOR-ricTOR complex 2 phosphorylates Ser⁴⁷³. Activated Akt translocates to the cytoplasmic region to control mTOR phosphorylation.

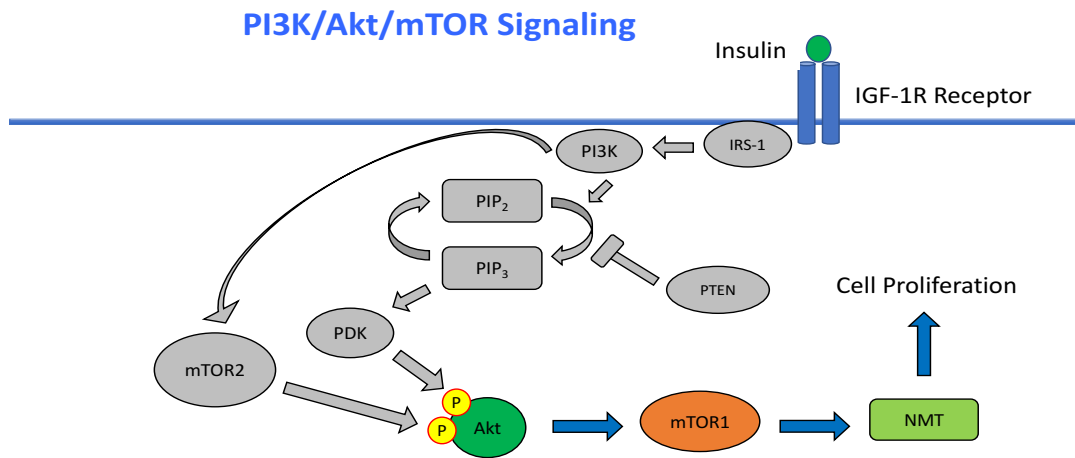


Figure 10. The PI3K/Akt/mTOR pathway plays an essential role in cell proliferation.

i. Regulation of mTOR: mTOR is a serine/threonine kinase that regulates protein synthesis and cell proliferation through phosphorylation of its downstream targets [45, 50]. Recent biochemical and genetic studies have demonstrated that mTOR exists in two different complexes referred to as mTOR-raptor complex 1 (mTORC1) and mTOR-riCTOR complex 2 (mTORC2). mTORC1 positively regulates cell proliferation, autophagy, and protein synthesis. mTOR activation following RTK stimulation can result in phosphorylation and activation of ribosomal protein S6 kinase (S6K), which leads to activation of S6 transcription factors. mTORC2 plays a key role in various biological processes, including: metabolism, cytoskeleton organization, and phosphorylation of Akt.

ii. Dysregulation of mTOR: mTOR plays a central role in the regulation of cell growth and proliferation. One downstream target of mTOR is p70^{S6K}, which then leads to the phosphorylation of 40S ribosomal S6 to initiate translation of mRNA [51], [52]. Dysregulation of mTOR activity manifests as abnormal cell growth. A protein that can decrease activity of mTOR is PTEN [53]. PTEN is a tumor suppressor that functions as a dual-specificity lipid and protein phosphatase that inhibits cell proliferation and the inactivation of other tumor suppressors. By dephosphorylation of PIP3 into PIP2, PTEN negatively regulates PI3K/Akt signaling and subsequent downstream pathways [51]. Regulating the PI3K/Akt/mTOR signaling pathway has been shown to be pivotal to prostate cancer proliferation and the pathogenesis of an advanced disease [54], [55].

NMT Activity in PI3K/Akt/mTOR pathway

NMT modifies proteins by covalently attaching a myristoyl group to their N-terminus. Activation of Akt/PKB, a central hub protein of the insulin signaling pathway, leads to the phosphorylation of NMT1. Our lab has previously shown that the mTOR and NMT based pathways are interlinked since NMT has been demonstrated to myristoylate mTOR and mTOR phosphorylates NMT.

Rapamycin Treatment

Rapamycin (Sirolimus) is a macrocyclic antibiotic that is produced by bacteria called *Streptomyces hygroscopicus* (Figure 11) [56]. It is used as an immunosuppressant, and its analog, RAD001, delays cell proliferation. Rapamycin and the rapalogue, RAD001, are used as tumor suppressive drugs in cancer treatments and are used as immunosuppressive drugs during organ transplants [56]. Rapamycin is known to inhibit mTOR, thus blocking the activity of its downstream targets (Figure 12). mTOR directed inhibition can take place via one of two mechanisms, competitive ATP-subunit inhibitors, or uncompetitive allosteric inhibitors. Rapamycin is an allosteric inhibitor that first binds with the intracellular receptor FKB12 and targets the FRB (FKBP12/rapamycin-binding) domain of mTORC1[56]. mTOR forms two major complexes: mTORC1, and mTORC2. The mTORC1 consists of mTOR, Raptor, mLST8, FKBP38, PRAS40, and Deptor. Compared to mTORC2, rapamycin inhibition is extremely selective for mTORC1. In early studies of mTOR, rapamycin was used almost entirely to describe the functions of mTOR, which it inhibits [57]. The inability of rapamycin and other rapalogues to inhibit mTORC2 has contributed to the lessened understanding regarding the cellular functions of this complex.

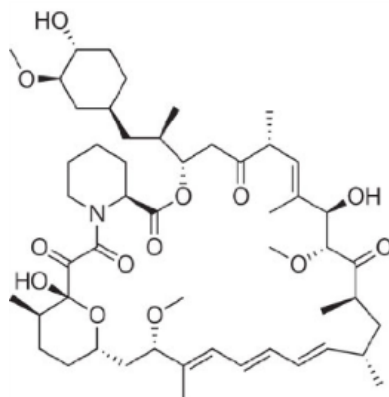


Figure 11. Rapamycin is a macrocyclic antibiotic that inhibits the highly conserved protein kinase target of rapamycin (TOR) by forming a complex with FKBP12, which then binds directly to mammalian TOR complex 1 (mTORC1) and inhibits mTOR pathway.

The proposed mechanism of rapamycin inhibition is postulated to be through the destabilization of the mTOR-raptor binding, resulting in the destabilization of the mTORC1 complex [56]. The major issue with inhibiting mTORC1 as a method of cancer treatment is the inherent nature of the negative feedback loop it controls. mTORC1 inhibition may lead to the development of an mTORC1 independent growth pathway with an upregulation of Akt, due to failure of inhibiting IRS-1/2 activity [58]. Mitigating strategies have been developed, such as using dual mTOR and PI3K inhibitors, and ATP-competitive inhibitors that inhibit both mTORC1 and mTORC2 have been developed as alternative cancer treatments [56].

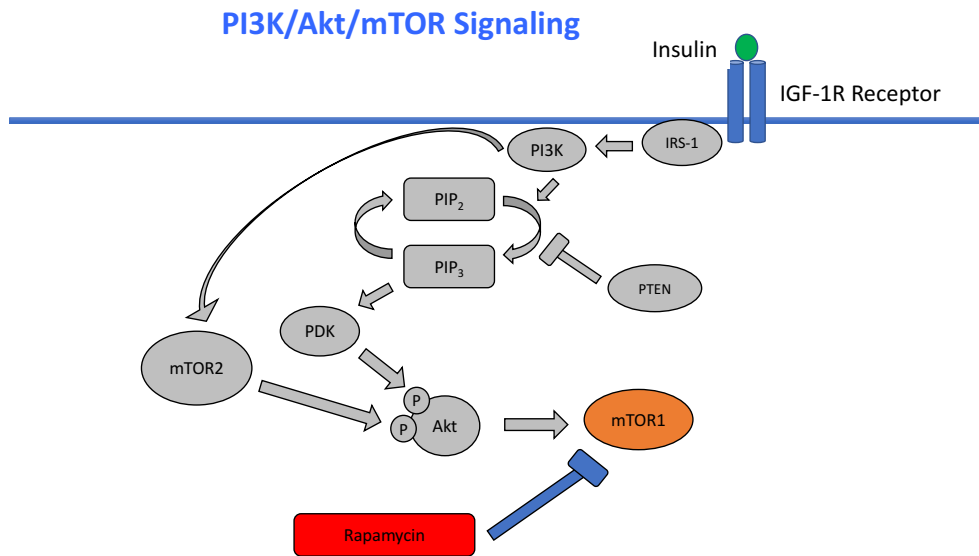


Figure 12. Rapamycin binds the intracellular receptor, interfering with growth-promoting cytokine signaling. This is done through inhibition of mTOR autophosphorylation and phosphorylation of initiation factor 4E binding protein, 4EBP1, which plays an important role in translation.

HYPOTHESIS

NMT1 regulates metabolic pathways.

OBJECTIVE

To investigate the effect of NMT deficiency on metabolic pathway.

MATERIALS AND METHODS

Generation of Heterozygous (*Nmt1*^{+/-}) and Homozygous (*Nmt1*^{-/-}) – deficient ES cells

Nmt1-deficient (*Nmt1*^{+/-} and *Nmt1*^{-/-}) ES cells were generated as described previously [59]. In brief, a mouse ES cell line (XE400, strain 129/Ola) with an insertional mutation in the *Nmt1* gene was created in a gene-trapping program, BayGenomics (baygenomics.ucsf.edu).

Isolation of Heterozygous (*Nmt1*^{+/-}) and Homozygous (*Nmt1*^{-/-}) – deficient ES cells

Nmt1-deficient ES cells were isolated as previously described [59]. In brief, *Nmt1* mutant ES cells were grown for 24 h in ES cell medium in a 100-mm gelatin-coated petri dish. Single colonies were picked and grown under G418 selection pressure (20 mg/ml). *Nmt1* mutant ES cells were validated by Western blotting and RT-PCR.

ESC Cell culture

Wild type (WT) and *Nmt1*-deficient ES cell lines were cultured in Glasgow minimum essential medium (GMEM) (Sigma-Aldrich) supplemented with 2 mM glutamine (Invitrogen Life Technologies), 1 mM sodium pyruvate, 1X nonessential amino acids, 10% (v/v) FBS, a 1/1000 dilution of 2-mercaptoethanol (ME) of stock solution, 500 Units/ml LIF (Leukemia Inhibitory Factor) in a 100-mm gelatin coated Petri dish. Cells were cultured at 37 °C/5% CO₂. For metabolic pathway analysis, ES cells were seeded in gelatin coated T25 culture flasks and cultured overnight at 37 °C in a CO₂ incubator. One day prior to ES cell stimulation, ES cells were serum starved overnight, followed by 10 nM insulin and 10 nM rapamycin treatment. ES cells were cultured in the presence or absence of treatments for the indicated time points, after which the cells were washed with ice cold 1X PBS. Thereafter, cell pellets were collected

and incubated in lysis buffer (50mM HEPES (pH 7.4), 150mM sucrose, 2 mM sodium orthovanadate, 10 mM sodium fluoride, 10 mM sodium pyrophosphate, 2 mM EGTA, 2 mM EDTA, 1% triton X-100, and 0.1% SDS), supplemented with 1 mM phenylmethylsulfonyl fluoride (PMSF) and 1% protease inhibitor cocktail for 10 minutes on ice. After incubation, the pellets were centrifuged at 1600 rpm for 5 minutes. The supernatant was collected and stored at -20 °C until further analysis.

Western Blotting's

Adherent cells ESC were washed with PBS on ice, and then lysed with ice-cold 1% SDS lysis buffer. The Bicinchoninic acid (BCA) kit (Pierce) was used to estimate protein concentration (all in duplicate) of cell lysates according to the manufacture's protocol. Protein concentration was read by measuring absorbance at $\lambda = 560$ nm on a Multiskan Ascent (Thermo Electron Corporation) plate reader. Thirty μ g of protein was mixed with SDS-PAGE sample buffer (0.2M Tris-HCl pH 6.8, 40% glycerol, 8% SDS, and 0.04% bromophenol blue) and heated at 95 °C for 5 mins. The samples were resolved on a 10% polyacrylamide gel ran on SDS-PAGE buffer in a Bio-Rad Mini-Protean Tetra cell. Samples were run through the stacking gel at 100 V until the samples lined up at the top of the stacking gel and then the voltage was increased to 150 V. The proteins were transferred onto a PVDF membrane (Biorad) at 120 V for 90 minutes. The membrane was incubated for an hour with blocking solution (5% non-fat dry milk dissolved in 1X PBS-containing 0.02% Tween 20) at room temperature. Blots were probed with specific polyclonal rabbit antibodies against PI3K p100 α , phosphorylated Akt, AMPK, mTOR, GSK and IGF1R diluted (1:1000) in 5% milk-PBST, overnight at 4 °C. The membrane was then washed in PBST three times for 10 min each followed by incubation with

suitable secondary antibody (1:2000) conjugated with horseradish peroxidase for 1 hour at room temperature. The membrane was washed in PBST three times for 10 min each; visualization was done using ClarityWestern ECL substrate (Bio-Rad) reagent and a Molecular Imager® ChemiDoc™ XRS System (Bio-Rad) and Image Lab™ software Version 3.0. Thereafter, the blots were routinely stripped and re-probed with antibodies against total Akt, AMPK, mTOR, GSK and IGF1R. that were used as loading controls. Densitometric analysis was performed and integrated density values were presented as ratio of phosphorylated protein over total compared with WT control.

RESULTS

1. NMT1 protein expression is completely abrogated in *Nmt1*^{-/-} ESC

In order to study the mechanism by which NMT1 activity impacts metabolic pathway, *Nmt1*^{-/-} KO cells were developed as described in materials. The successful ablation of *Nmt1* was validated by qPCR and Western blot analysis [41]. Western blot analysis revealed the complete absence of NMT1 protein expression in homozygous KO cells and almost 50% ablation in heterozygous cells whereas β -actin, which was used as the loading control, was similar in *Nmt1*^{+/+}, *Nmt1*^{+/-} and *Nmt1*^{-/-} KO ES cells. Relative normalized *Nmt1* gene expression was assessed by RT-PCR in *Nmt1*^{+/+} ES, *Nmt1*^{+/-} and WT ES cells (Figure 13B). We also validated NMT1 protein expression using both commercially available antibodies and custom monoclonal antibodies raised in a murine system (Figure 13A).

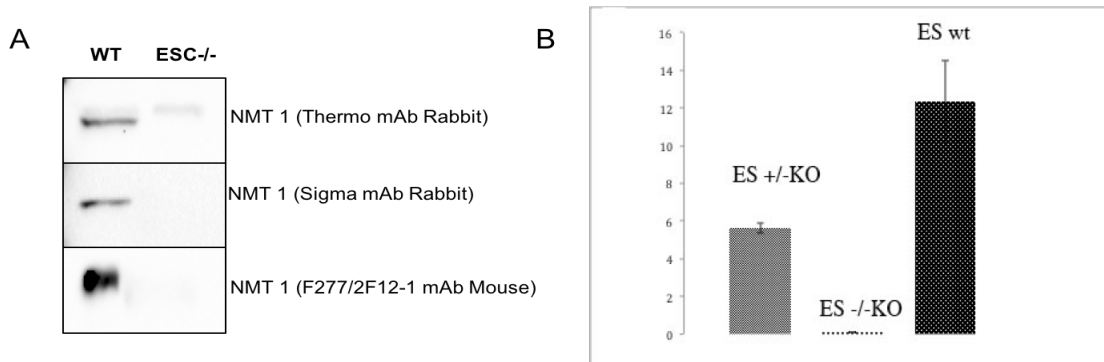


Figure 13. NMT1 protein expression by Western blot was assessed in WT ES and *Nmt1*^{-/-} ES cells by different antibodies (Figure 13A). Relative normalized *Nmt1* gene expression was assessed by RT-PCR in *Nmt1*^{+/+} ES, *Nmt1*^{+/-} and WT ES cells (Figure 13B).

2. PI3K p110 α expression is up-regulated in *Nmt1*^{-/-} ESC

Growth factors such as insulin, epidermal growth factors, nerve growth factors and platelet derived growth factors bind to cell surface transmembrane receptors

belonging to the RTK superfamily and regulate metabolic pathways. A major downstream hub of I/IGF1R pathway is PI3K/Akt, therefore, the effect of NMT1 ablation was investigated on metabolic pathway regulated by PI3K/Akt compounded with the fact that NMT1 is a downstream target of Akt [43]. For this, I used embryonic stem (ES) cells from *Nmt1*^{-/-} knockout mice, and these cells were subjected to different treatments to modulate insulin signaling. The ES cells were treated with insulin to activate the RTK and its downstream target proteins, and with rapamycin to inhibit mTOR. Thereafter, a combination of rapamycin pretreatment, followed by insulin treatment was also given to assess the effect of mTOR inhibition on the activation of RTK and downstream targets. The phosphatidylinositol-4,5-bisphosphate 3-kinase, catalytic subunit alpha (p110 α) is a major regulator of PI3K/Akt pathway; therefore, I first investigated the effect of *Nmt1*^{-/-} knockout on p110 α expression. As shown in Figure 14, NMT1 WT ES cells showed p110 α basal expression and different treatments had no effect on the basal expression. However, *Nmt1*^{-/-} ES cells showed increased p110 α expression, and activation of the pathway with insulin or rapamycin further enhanced p110 α expression. The same membrane was probed with anti-NMT1 antibody to confirm that *Nmt1*^{-/-} ES cells were deficient in NMT1. Figure 14C shows the NMT1 expression in WT and *Nmt1*^{-/-} ES cells in the same blot that was probed with Akt.

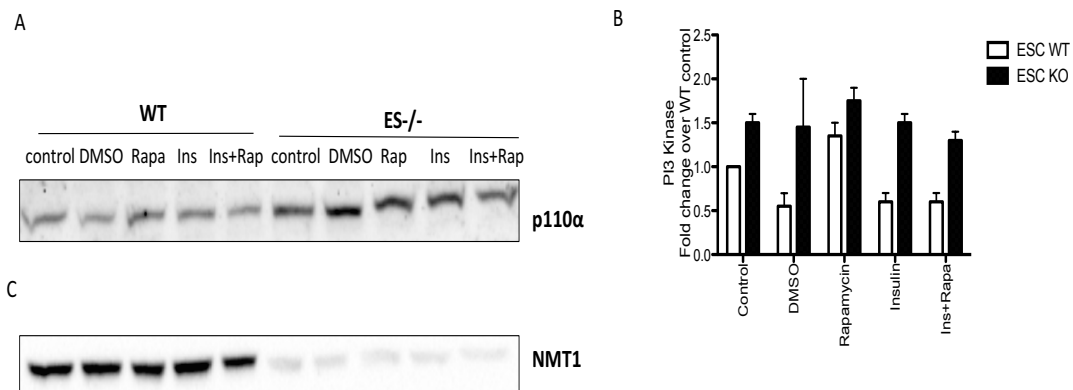


Figure 14. *Nmt1*^{-/-} ES cells show increased PI3K p110 α expression. WT ES and *Nmt1*^{-/-} ES cells were treated with rapamycin (10 nM) and/or insulin (100 nM) for 24 hrs. The cells were lysed and the lysates were assessed by Western blot for the expression of the catalytic subunit of PI3K, p110 α (Figure 14A). The right panel shows the corresponding densitometry (Figure 14B). The same membrane was stripped and reprobbed with NMT1 (Figure 14C).

3. Akt phosphorylation is up regulated in *Nmt1*^{-/-} ES cells compared to WT ESC

Previously it has been demonstrated that overexpression of Akt/PKB resulted in the phosphorylation of NMT1 in breast cancer cells [60] establishing NMT1 as a downstream target of Akt. Therefore, I determined the effect of different treatments on the phosphorylation of Akt in WT and *Nmt1*^{-/-} ES cells. As shown in (Figure 15A), WT ES cells showed decrease in the phosphorylation of Akt compared to *Nmt1*^{-/-} ES cells. Interestingly, phosphorylation of Akt at Ser⁴⁷³ was significantly upregulated upon treatment with insulin alone in *Nmt1*^{-/-} KO cells.

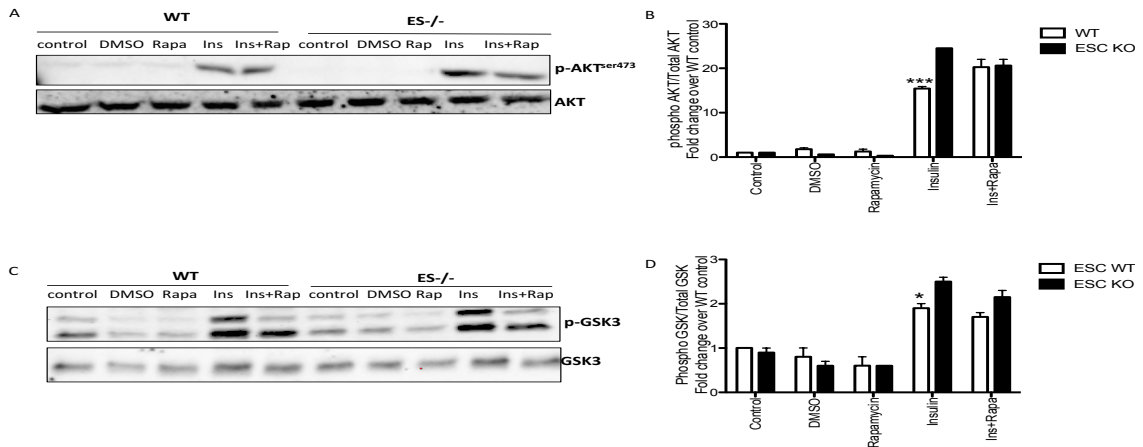


Figure 15. Akt and GSK phosphorylation was upregulated in *Nmt1*^{-/-} ES cells upon insulin treatment. WT ES and *Nmt1*^{-/-} ES cells were treated with rapamycin (10nM) and/or insulin (100nM) for 24 hrs. The cells were lysed and the lysates were assessed by western blot for the phosphorylation of Akt (Figure 15A) and GSK3 (Figure 15C). The same blots were stripped and re-probed with Abs against total Akt and GSK3 and used as loading controls. The right panel shows the corresponding densitometry (Figure 15B and 15D). The Western blot results represent one of three independent experiments with similar findings.

4. GSK phosphorylation is up regulated in *Nmt1*^{-/-} ES cells compared to WT ESC

Remarkable up-regulation of p110 α and AKT in *Nmt1*^{-/-} KO ES cells prompted me to further investigate two key regulators of metabolic pathways – glycogen synthase kinase 3 (GSK3) and mTOR (Figure 15). Although GSK3 was initially identified in the regulation of glycogen synthesis, it has been shown that GSK3 plays a role in a wide range of cellular processes particularly in cancer [61]. The GSK3 gene family has two highly conserved kinases including GSK3 α and GSK3 β . Both kinases are structurally similar but not identical in terms of their functions [61]. Figure 15D shows the expression of GSK 3 α / β . GSK3 α / β . phosphorylation was upregulated upon treatment with insulin alone or in combination with rapamycin in *Nmt1*^{-/-} ES cells compared to WT cells.

5. mTOR phosphorylation is up regulated in *Nmt1*^{-/-} ES cells compared to WT ESC

mTOR is a downstream target of the PI3K/Akt pathway and is the central regulator of protein synthesis and metabolism [62]. Therefore, we determined the expression of total mTOR and its phosphorylation at the Ser²⁴⁴⁸ residue (Figure 16A). In WT ES cells, the total mTOR expression did not change upon treatment with insulin and/or rapamycin. However, the phosphorylation of mTOR Ser²⁴⁴⁸ was downregulated upon rapamycin treatment in WT cells whereas the mTOR phosphorylation was greater in *Nmt1*^{-/-} ES cells and was further enhanced upon treatment with insulin. In line with what I observed for other PI3K pathway proteins, NMT1 deficiency is associated with increased mTOR phosphorylation.

6. *Nmt1*^{-/-} ES cells show increased IGF1R phosphorylation compared to WT ESC

Insulin like growth factor 1 and 2 binds to type 1 insulin like growth factor receptor and activates the downstream signaling pathways. Insulin receptor substrates IRS1 and IRS2 are the main adaptors that act as docking sites and link the activated receptors to various intracellular adaptor proteins and downstream signaling cascades including PI3K/Akt signaling cascades [63, 64]. Insulin-like growth factor is important in mammary development and IGF1R is required for mammary gland morphogenesis. Although IGF1 plays a critical role in cell growth, survival and migration several studies have shown that alterations in the IGF signaling results in the development and progression of multiple cancers. Since increased p110 α expression and increased phosphorylation of Akt and mTOR were observed due to NMT1 ablation, I wanted to investigate whether the IGF1R phosphorylation is affected in WT and in *Nmt1*^{-/-} ES cells.

Therefore I treated both, the WT and *Nmt1*^{-/-} ES cells, with insulin and rapamycin and assessed the phosphorylation. Interestingly, IGF1R phosphorylation was upregulated in the *Nmt1*^{-/-} ES cells compared to WT cells (Figure 16C).

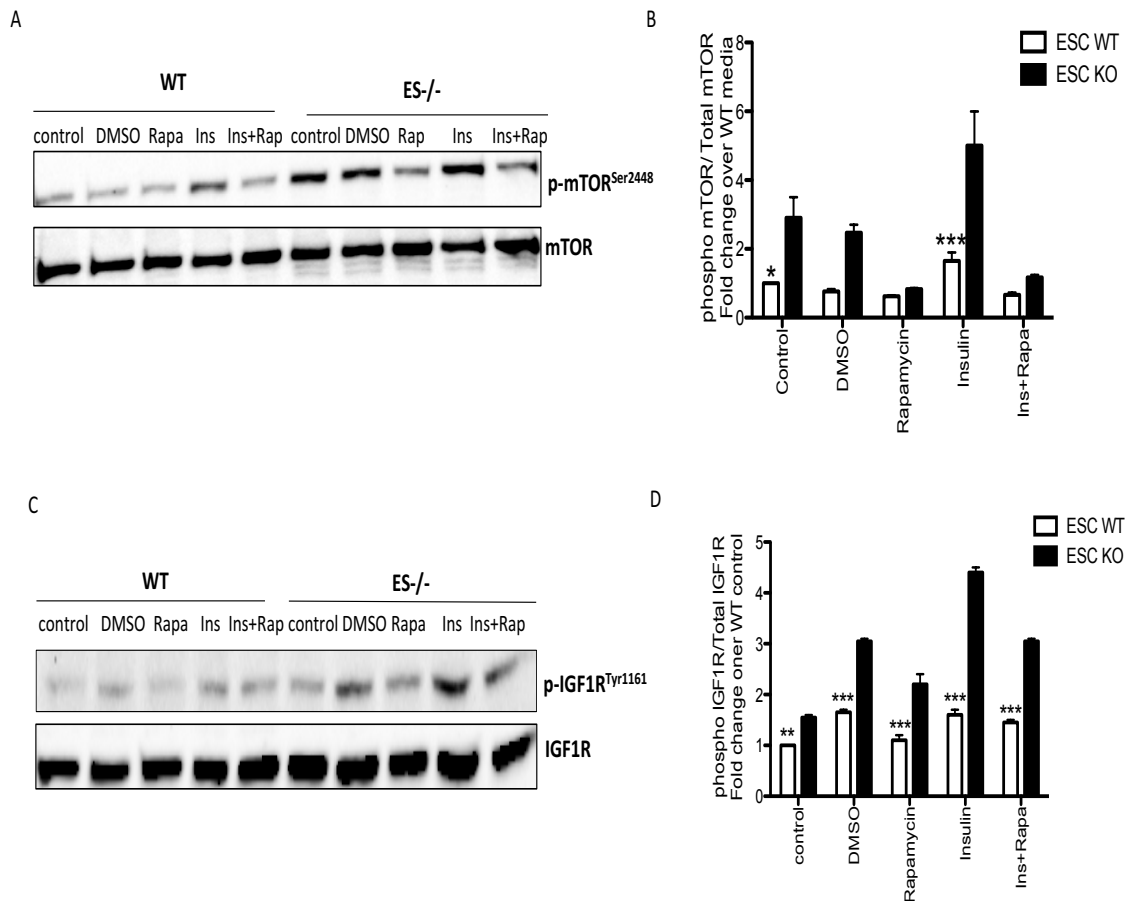


Figure 16. mTOR and IGF1R phosphorylation was upregulated in *Nmt1*^{-/-} ES cells compared to WT cells. WT ES and *Nmt1*^{-/-} ES cells were treated with rapamycin (10nM) and/or insulin (100nM) for 24 hrs. The cells were lysed and the lysates were assessed by Western blot for the phosphorylation of mTOR (Figure 16A) and IGF1R (Figure 16C). The same blots were stripped and re-probed with Abs against total mTOR and IGF1R and used as loading controls. The right panel shows the corresponding densitometry (Figure 16B and 16D). The Western blot results represent one of three independent experiments with similar findings.

7. AMPK phosphorylation is upregulated in WT cells compared to *Nmt1*^{-/-} ESC

AMP activated protein kinase (AMPK) is a heterotrimeric enzyme consisting of one catalytic subunit and two regulatory subunits. Reports have shown that AMPK regulates IRS1 and Akt whereas insulin and Akt are shown to have negative impacts on AMPK activation [65-67]. In Figure 17, we were interested to see the effect of NMT1 deficiency on AMPK phosphorylation. Unlike the other signaling molecules, AMPK phosphorylation was upregulated in WT cells compared to *Nmt1*^{-/-} ES cells.

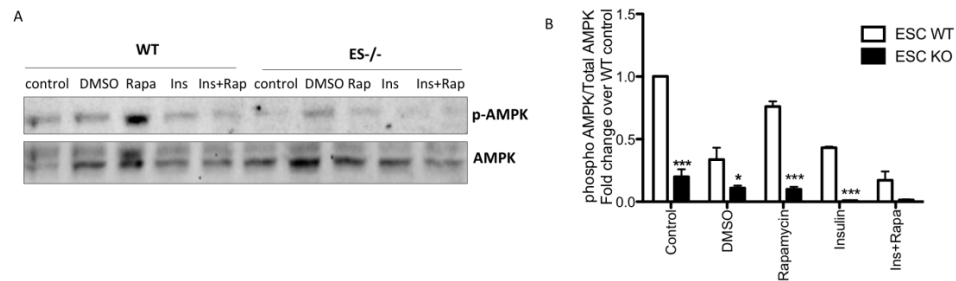


Figure 17. AMPK phosphorylation was upregulated in WT ES cells compared to *Nmt1*^{-/-} ESC cells.

DISCUSSION

N-myristoylation is an important protein modification that regulates protein function and localization. Myristoylated proteins have shown to be involved in various cellular processes, including cellular proliferation and oncogenesis [13]. Evidence from various studies suggests the involvement of NMT in cancer development and progression [25]. In the present study, I attempted to identify whether NMT deficiency has any impact on the PI3K-Akt signaling pathway. Several reports have shown that the PI3K-Akt signaling pathway proteins involved in cell growth and differentiation undergo oncogenic changes and are altered in various human cancers. This pathway plays a critical role in tumor development as well as in the potential response of tumor to cancer treatment.

The results of this study identify for the first time how the deficiency of NMT1 affects the key PI3K-Akt pathway signaling proteins. The class IA PI3K forms an important node in the insulin metabolic pathway. It was observed that in the absence of NMT1, p110 α protein expression was upregulated and all subsequent downstream targets such as Akt, mTOR, GSK3 and IGF1R phosphorylation was also increased following insulin treatment.

The Wilm's tumor 1 protein (WT1) has been shown to be a transcriptional regulator that can either activate or repress transcription of key growth factors [68]. WT1 functions as an activator on its own, but its binding to the BASP1 corepressor shifts WT1 activity to a state of transcriptional repression [69]. BASP1 has been identified as a WT1-

binding protein, which mediates the transcriptional repression activity of the latter [70]. Translocation of transcription factors is important for the regulation of gene expression. Many transcription factors, such as BASP1 are myristoylated and several studies have shown that BASP1 is stoichiometrically N-terminally myristoylated in different tissues [71]. Myristoylation is required for the binding of BASP1 to WT1 [69]. It has been demonstrated that *IGF1R* gene expression is regulated by WT1 [72], which indirectly suggests the possibility of NMT1 involvement in *IGF1R* gene expression/regulation. When BASP1 and WT1 are joined in a complex, WT1 acts as a transcriptional repressor that inhibits *IGF1R* gene expression. This increase in *IGF1R* gene expression could be the reason for over activation of the IGF1R signaling pathway proteins observed in *Nmt1*^{-/-} ES cells.

I observed that NMT1 deficiency has a direct effect on overall protein expression (Figures 7-9). NMT1 deficiency resulted in the activation of PI3K/AKT pathway upon treatment with Rapamycin and Insulin. GSK3 has been shown to regulate the activities of certain transcription factors such as NF-kappaB, Snail, Notch and CAAT-enhancer binding protein (C/EBP) [73-75]. Even after several years of research, the role of GSK3 in cancer remains complex and controversial. GSK3 has shown to be overexpressed in various cancers including that of colon, liver, ovarian and pancreatic tumors [76-78]. Our results show an increase in GSK3 phosphorylation in *Nmt1*^{-/-} ES cells compared to WT cells, suggesting that in the absence of NMT1, no myristoylation occurs and therefore there is no complex formation between BASP1 and WT1, which in turn leads to increased IGF1R expression due to the lack of repressor activity.

CONCLUSION

In summary, a precise balance between growth promoting signals and growth inhibitory signals plays important roles in the maintenance of healthy cells. Any dysregulation of this critical balance converts normal cells into abnormal or cancerous cells. In chapter one, RT-PCR analysis show that *NMT1* and *METAP2* transcripts are overexpressed in CRC patients' whole blood and PBMC. Both *NMT1* and *METAP2* were the highest in CRC compared to healthy controls, non-adenomatous polyps, and adenomatous polyps. In addition, an increase in *METAP2* than *NMT1* activity appeared in adenomatous polyp. The results of my study provide insight into effect of *NMT1* and *METAP2* overexpression on immune response PBMC as they play important role in tumor progression. Therefore, *METAP2* can be used as a potential marker for the early detection of colorectal cancer. These observations lead to the possibility of developing *MetAP2* specific inhibitors, which may be therapeutically useful. RT-PCR method is a convenient, more accurate and cost-effective screening test that could triage patients for more intensive procedures such as colonoscopy. The outcome of my study could lead to development of an efficacious screening test for CRC.

In the last chapter, Western blot analysis revealed that ESC *Nmt1*^{-/-} KO has an over activation of the PI3K/Akt pathway compared to WT ESC. This pathway is essential for cellular growth, and cell proliferation. In the absence of NMT1, the downstream targets: p110 α subunit of PI3K, Akt, GSK3, mTOR, and IGF1R were all upregulated.

However, AMPK levels were downregulated in NMT1^{-/-} ES cells. In addition to Western blots, I observed the ESC *Nmt1*^{-/-} KO cell line was proliferating faster than WT. NMT1 is vital for proper function cell division. The macroscopic result reveals that when NMT1 not present, the P13K/Akt pathway is overactive and induce cell proliferation. It is possible that overexpression of NMT1 in PBMC of individuals with polyps and CRC may be one of the reasons for their lower PBMC proliferation [79].

Overall, the results from RT-PCR and Western blot demonstrate development of rational combinations, driven by compelling preclinical data and matched to genetic drivers in patients. This study has the potential to significantly improve the future care of cancer patients. The outcome of my study would lead to the development of an efficacious screening test for CRC.

REFERENCE

1. Public Health Agency of, C., C. Statistics, and S. Canadian Cancer, *Canadian cancer statistics 2010 special topic : end-of-life care*. 2010.
2. Society, A.C. *American Cancer Society*. Cancer Facts & Figures 2018 2018.
3. Scholefield, J. and C. Eng, *Colorectal Cancer : Diagnosis and Clinical Management*. 2014, Wiley: Hoboken :.
4. Beauchemin, N. and J. Huot, *Metastasis of colorectal cancer*. 2010, Springer: Dordrecht ;.
5. Elk, R. and H. Landrine, *Cancer disparities : causes and evidence-based solutions*. 2012, Springer Pub.: New York :.
6. Jemal, A., et al., *Global cancer statistics*. CA: A Cancer Journal for Clinicians, 2011. **61**(2): p. 69-90.
7. Moayyedi, P., *Colorectal cancer screening lacks evidence of benefit*. Cleveland Clinic journal of medicine, 2007. **74**(8): p. 549-50.
8. Selvakumar P, L.A., Shrivastav A, Dimmock JR, Sharma RK, *Myristoylation and cell signalling: involvement of heat shock protein 70 family*. Recent Dev Life Sci, 2005(3): p. 75–82.
9. Resh, M.D., *Fatty acylation of proteins: new insights into membrane targeting of myristoylated and palmitoylated proteins*. Biochim Biophys Acta, 1999. **1451**(1): p. 1-16.
10. Boutin, J.A., *Myristoylation*. Cell Signal, 1997. **9**(1): p. 15-35.
11. Farazi, T.A., G. Waksman, and J.I. Gordon, *The biology and enzymology of protein N-myristoylation*. J Biol Chem, 2001. **276**(43): p. 39501-4.
12. Shrivastav, A., et al., *Regulation of N-myristoyltransferase by novel inhibitor proteins*. Cell Biochem Biophys, 2005. **43**(1): p. 189-202.
13. Bajaj, G., Shrivastav, A., Selvakumar, P., Pasha, M.K., Lu, Y., Dimmock, J.R., Sharma, R.K., *Inhibitors of NMT: a new class of chemotherapeutic drugs*. Drug Design Reviews-Online, 2004. **1**: p. 347-354.
14. Carr, S.A., et al., *n-Tetradecanoyl is the NH₂-terminal blocking group of the catalytic subunit of cyclic AMP-dependent protein kinase from bovine cardiac muscle*. Proc Natl Acad Sci U S A, 1982. **79**(20): p. 6128-31.
15. Aitken, A., et al., *Identification of the NH₂-terminal blocking group of calcineurin B as myristic acid*. FEBS Lett, 1982. **150**(2): p. 314-8.
16. Schultz, A.M., et al., *Hydroxylamine-stable covalent linkage of myristic acid in G0 alpha, a guanine nucleotide-binding protein of bovine brain*. Biochem Biophys Res Commun, 1987. **146**(3): p. 1234-9.
17. Schultz, A.M., et al., *Amino terminal myristylation of the protein kinase p60src, a retroviral transforming protein*. Science, 1985. **227**(4685): p. 427-9.
18. Selvakumar, P., et al., *Potential role of N-myristoyltransferase in cancer*. Progress in Lipid Research, 2007. **46**(1): p. 1-36.
19. Magnuson, B.A., et al., *Increased N-Myristoyltransferase Activity Observed in Rat and Human Colonic Tumors*. JNCI Journal of the National Cancer Institute, 1995. **87**(21): p. 1630-1635.
20. Sharma, R., *Potential role of N-myristoyltransferase in pathogenic conditions*. Canadian Journal of Physiology and Pharmacology, 2004. **82**: p. 849-859.

21. Lowther, W.T. and B.W. Matthews, *Structure and function of the methionine aminopeptidases*. Biochimica et Biophysica Acta (BBA) - Protein Structure and Molecular Enzymology, 2000. **1477**(1): p. 157-167.
22. Frottin, F., et al., *MetAP1 and MetAP2 drive cell selectivity for a potent anti-cancer agent in synergy, by controlling glutathione redox state*. Oncotarget, 2016. **7**(39): p. 63306-63323.
23. Selvakumar, P., et al., *High expression of methionine aminopeptidase 2 in human colorectal adenocarcinomas*. Clinical cancer research : an official journal of the American Association for Cancer Research, 2004. **10**(8): p. 2771-5.
24. Anuraag, S., et al. *N-myristoyltransferase: A potential novel diagnostic marker for colon cancer*. Journal of Translational Medicine, 2007. **5**, 58.
25. Kumar, S., et al., *N-myristoyltransferase in the leukocytic development processes*. Cell and tissue research, 2011. **345**(2): p. 203-11.
26. Désert, C., et al., *Transcriptomes of whole blood and PBMC in chickens*. Comparative Biochemistry and Physiology Part D: Genomics and Proteomics, 2016. **20**: p. 1-9.
27. Vergara, D., et al., *Proteomic map of peripheral blood mononuclear cells*. PMIC PROTEOMICS, 2008. **8**(10): p. 2045-2051.
28. Livak, K.J. and T.D. Schmittgen, *Analysis of Relative Gene Expression Data Using Real-Time Quantitative PCR and the 2⁻ $\Delta\Delta$ CT Method*. Methods, 2001. **25**(4): p. 402-408.
29. Tabatabaeian, H. and Z. Hojati, *Assessment of HER-2 gene overexpression in Isfahan province breast cancer patients using Real Time RT-PCR and immunohistochemistry*. Gene, 2013. **531**(1): p. 39-43.
30. Abe, J., et al., *A fumagillin derivative angiogenesis inhibitor, AGM-1470, inhibits activation of cyclin-dependent kinases and phosphorylation of retinoblastoma gene product but not protein tyrosyl phosphorylation or protooncogene expression in vascular endothelial cells*. Cancer research, 1994. **54**(13): p. 3407-12.
31. Kanno, T., et al., *High expression of methionine aminopeptidase type 2 in germinal center B cells and their neoplastic counterparts*. Laboratory investigation; a journal of technical methods and pathology, 2002. **82**(7): p. 893-901.
32. Hayat, M.A. and SpringerLink, *Stem cells and cancer stem cells. Volume 11, Therapeutic applications in disease and injury*. 2014, Springer: Dordrecht .
33. Notarianni, E. and M.J.P. Evans, *Embryonic stem cells : a practical approach*. 2006, Oxford University Press: Oxford ;.
34. Takahashi, F., et al., *Regulation of cell-cell contacts in developing Drosophila eyes by Dsrc41, a new, close relative of vertebrate c-src*. Genes Dev, 1996. **10**(13): p. 1645-56.
35. Kussick, S.J., K. Basler, and J.A. Cooper, *Ras1-dependent signaling by ectopically-expressed Drosophila src gene product in the embryo and developing eye*. Oncogene, 1993. **8**(10): p. 2791-803.
36. Ntwasa, M., et al., *Drosophila embryos lacking N-myristoyltransferase have multiple developmental defects*. Exp Cell Res, 2001. **262**(2): p. 134-44.

37. Giang, D.K. and B.F. Cravatt, *A second mammalian N-myristoyltransferase*. J Biol Chem, 1998. **273**(12): p. 6595-8.
38. Raju, R.V., T.N. Moyana, and R.K. Sharma, *N-Myristoyltransferase overexpression in human colorectal adenocarcinomas*. Experimental cell research, 1997. **235**(1): p. 145-54.
39. Giang, D.K. and B.F. Cravatt, *A second mammalian N-myristoyltransferase*. The Journal of biological chemistry, 1998. **273**(12): p. 6595-8.
40. Yang, S.H., et al., *N-myristoyltransferase 1 is essential in early mouse development*. The Journal of biological chemistry, 2005. **280**(19): p. 18990-5.
41. Shrivastav, A., et al., *Requirement of N-myristoyltransferase 1 in the development of monocytic lineage*. Journal of immunology, 2008. **180**(2): p. 1019-28.
42. Shrivastav, A., et al., *Expression and activity of N-myristoyltransferase in lung inflammation of cattle and its role in neutrophil apoptosis*. Veterinary research, 2010. **41**(1): p. 9.
43. Shrivastav, A., et al., *Overexpression of Akt/PKB modulates N-myristoyltransferase activity in cancer cells*. The Journal of Pathology, 2009. **218**(3): p. 391-398.
44. Johnson, D.E., *Cell death signaling in cancer biology and treatment*. 2013.
45. Schatz, J.H., *Targeting the PI3K/AKT/mTOR Pathway in Non-Hodgkin's Lymphoma: Results, Biology, and Development Strategies*. Current Oncology Reports, 2011. **13**(5): p. 398-406.
46. Choi, S., *Encyclopedia of signaling molecules*. 2012.
47. Bibollet-Bahena, O. and G. Almazan, *IGF-1-stimulated protein synthesis in oligodendrocyte progenitors requires PI3K/mTOR/Akt and MEK/ERK pathways*. JNC Journal of Neurochemistry, 2009. **109**(5): p. 1440-1451.
48. Polivka, J., Jr. and F. Janku, *Molecular targets for cancer therapy in the PI3K/AKT/mTOR pathway*. Pharmacology & therapeutics, 2014. **142**(2): p. 164-75.
49. Mitra, A., S.K. Raychaudhuri, and S.P. Raychaudhuri, *IL-22 induced cell proliferation is regulated by PI3K/Akt/mTOR signaling cascade*. Cytokine, 2012. **60**(1): p. 38-42.
50. Arsham, A.M. and T.P. Neufeld, *Thinking globally and acting locally with TOR*. Current Opinion in Cell Biology, 2006. **18**(6): p. 589-597.
51. Wolin, E.M., *PI3K/Akt/mTOR pathway inhibitors in the therapy of pancreatic neuroendocrine tumors*. Cancer letters, 2013. **335**(1): p. 1-8.
52. Burris, H.A., 3rd, *Overcoming acquired resistance to anticancer therapy: focus on the PI3K/AKT/mTOR pathway*. Cancer chemotherapy and pharmacology, 2013. **71**(4): p. 829-42.
53. Lau, M.T. and P.C. Leung, *The PI3K/Akt/mTOR signaling pathway mediates insulin-like growth factor 1-induced E-cadherin down-regulation and cell proliferation in ovarian cancer cells*. Cancer letters, 2012. **326**(2): p. 191-8.
54. Sauer, S., et al., *T cell receptor signaling controls Foxp3 expression via PI3K, Akt, and mTOR*. Proceedings of the National Academy of Sciences of the United States of America, 2008. **105**(22): p. 7797-802.

55. Saini, K.S., et al., *Targeting the PI3K/AKT/mTOR and Raf/MEK/ERK pathways in the treatment of breast cancer*. Cancer treatment reviews, 2013. **39**(8): p. 935-46.
56. Ballou, L.M. and R.Z. Lin, *Rapamycin and mTOR kinase inhibitors*. Journal of Chemical Biology, 2008. **1**(1-4): p. 27-36.
57. Varma, S., et al., *Long-term effects of rapamycin treatment on insulin mediated phosphorylation of Akt/PKB and glycogen synthase activity*. Experimental cell research, 2008. **314**(6): p. 1281-91.
58. Li, J., S.G. Kim, and J. Blenis, *Rapamycin: one drug, many effects*. Cell metabolism, 2014. **19**(3): p. 373-379.
59. Yang, S.H., et al., *N-myristoyltransferase 1 is essential in early mouse development*. J Biol Chem, 2005. **280**(19): p. 18990-5.
60. Shrivastav, A., et al., *Overexpression of Akt/PKB modulates N-myristoyltransferase activity in cancer cells*. J Pathol, 2009. **218**(3): p. 391-8.
61. McCubrey, J.A., et al., *GSK-3 as potential target for therapeutic intervention in cancer*. Oncotarget, 2014. **5**(10): p. 2881-911.
62. Laplante, M. and D.M. Sabatini, *mTOR signaling in growth control and disease*. Cell, 2012. **149**(2): p. 274-93.
63. Myers, M.G., Jr., et al., *IRS-1 is a common element in insulin and insulin-like growth factor-I signaling to the phosphatidylinositol 3'-kinase*. Endocrinology, 1993. **132**(4): p. 1421-30.
64. Dearth, R.K., et al., *Mammary tumorigenesis and metastasis caused by overexpression of insulin receptor substrate 1 (IRS-1) or IRS-2*. Mol Cell Biol, 2006. **26**(24): p. 9302-14.
65. Jakobsen, S.N., et al., *5'-AMP-activated protein kinase phosphorylates IRS-1 on Ser-789 in mouse C2C12 myotubes in response to 5-aminoimidazole-4-carboxamide riboside*. J Biol Chem, 2001. **276**(50): p. 46912-6.
66. Tzatsos, A. and P.N. Tsichlis, *Energy depletion inhibits phosphatidylinositol 3-kinase/Akt signaling and induces apoptosis via AMP-activated protein kinase-dependent phosphorylation of IRS-1 at Ser-794*. J Biol Chem, 2007. **282**(25): p. 18069-82.
67. Hahn-Windgassen, A., et al., *Akt activates the mammalian target of rapamycin by regulating cellular ATP level and AMPK activity*. J Biol Chem, 2005. **280**(37): p. 32081-9.
68. Roberts, S.G., *Transcriptional regulation by WTI in development*. Curr Opin Genet Dev, 2005. **15**(5): p. 542-7.
69. Toska, E., et al., *Repression of transcription by WTI-BASPI requires the myristoylation of BASPI and the PIP2-dependent recruitment of histone deacetylase*. Cell Rep, 2012. **2**(3): p. 462-9.
70. Carpenter, B., et al., *BASPI is a transcriptional cosuppressor for the Wilms' tumor suppressor protein WTI*. Mol Cell Biol, 2004. **24**(2): p. 537-49.
71. Mosevitsky, M.I., *Nerve ending "signal" proteins GAP-43, MARCKS, and BASPI*. Int Rev Cytol, 2005. **245**: p. 245-325.
72. Werner, H., et al., *Transcriptional repression of the insulin-like growth factor I receptor (IGF-I-R) gene by the tumor suppressor WTI involves binding to*

- sequences both upstream and downstream of the IGF-I-R gene transcription start site.* J Biol Chem, 1994. **269**(17): p. 12577-82.
73. Mishra, R., *Glycogen synthase kinase 3 beta: can it be a target for oral cancer.* Mol Cancer, 2010. **9**: p. 144.
 74. Haraguchi, M., et al., *Snail regulates cell-matrix adhesion by regulation of the expression of integrins and basement membrane proteins.* J Biol Chem, 2008. **283**(35): p. 23514-23.
 75. Ross, S.E., et al., *Glycogen synthase kinase 3 is an insulin-regulated C/EBPalpha kinase.* Mol Cell Biol, 1999. **19**(12): p. 8433-41.
 76. Luo, J., *Glycogen synthase kinase 3beta (GSK3beta) in tumorigenesis and cancer chemotherapy.* Cancer Lett, 2009. **273**(2): p. 194-200.
 77. Ougolkov, A.V., et al., *Glycogen synthase kinase-3beta participates in nuclear factor kappaB-mediated gene transcription and cell survival in pancreatic cancer cells.* Cancer Res, 2005. **65**(6): p. 2076-81.
 78. Shakoori, A., et al., *Deregulated GSK3beta activity in colorectal cancer: its association with tumor cell survival and proliferation.* Biochem Biophys Res Commun, 2005. **334**(4): p. 1365-73.
 79. Evans, C.F., et al., *The effect of colorectal cancer upon host peripheral immune cell function.* Colorectal disease : the official journal of the Association of Coloproctology of Great Britain and Ireland, 2010. **12**(6): p. 561-9.

APPENDICES

Appendix A: To maintain ESC media

Cell Type	LIF (10ng/ml) = 5 μ l	G418 (50mg/ml) = 20 μ l
ESC wild-type	Yes	No
ESC <i>Nmt1</i> ^{-/-} KO	Yes	Yes

Western Blot Assay

Treatment	Concentration
DMSO	10nM
Rapamycin	10nM
Insulin	100nM

To dilute 2-Mercaptoethanol Stock Solution

For ESC media (GMEM media)

35ul (2-mercaptoethanol) + 10ml (Ultrapure Distilled Water RNase and DNase free)

To make incomplete 1L of ESC Media (check if L-glutamine is added)

1. 12.5g (GMEM powder)
2. 2.75g (Sodium Bicarbonate NaHCO₃)
3. 800ml (Distilled Water)
4. Adjust pH 7.2-7.4
5. Add the remaining distilled water, Final volume = 1L
6. **Note make 5L instead of 1L**

Filter Sterilize: using a 2 micron vacuum filter before use

To make Complete 1L of ESC Media

1. 900ml (Incomplete-GMEM media)
2. 10ml (Sodium Pyruvate 100mM) → 1mM

3. 10ml (Non-essential amino acid 100X) → 1X
4. 100ml (FBS: Fetal bovine serum) → 10%
5. 1ml (B-mercaptoethanol Stock Solution) → 1:1000
6. 5ul (LIF 10ng/ml) per 10ml media
7. 20ul (G418 50mg/ml) **only for ESC Homo**

Appendix B: 0.05% Trypsin-EDTA (5mL)

- 1 mL 0.25% Trypsin-EDTA (1X), Phenol Red
- 4mL phosphate buffered saline

Appendix C: PBS (10X) (1 Litre)

- 80 g NaCl
- 2 g KCl
- 14.4 g Na₂HPO₄
- 2.4 g KH₂PO₄
- Dissolve all components in 800 mL R/O water
- Adjust pH to 7.4 using HCl or NaOH and bring final volume to 1000 mL

Appendix D: Lysis Buffer Preparation for Phosphoproteins (500 mL)

- 50 mM HEPES (pH 7.4) (5.975 g)
- 150 mM sucrose (25.67 g)
- 2 mM sodium orthovanadate (5 mL from 200 mM stock)*
- 80 mM glycerophosphate (12.24 g)
- 10 mM sodium fluoride (0.21 g)
- 10 mM sodium pyrophosphate (2.23 g)
- 2 mM EGTA (2 ml from 0.5M stock)**
- 2 mM EDTA (2 ml from 0.5M stock)***

- 1% TritonX-100 (5 mL)
- 0.1% SDS (0.5 g)
- 20 µl Phenylmethylsulfonyl fluoride (100 mM)**add fresh to 1 mL lysis buffer
- 20 µl protease inhibitor cocktail – add fresh to 1 mL lysis buffer

***Activation of sodium orthovanadate (Na₃VO₄)**

(to achieve maximal inhibition of protein tyrosine phosphatases)

1. Prepare 200 mM solution of sodium orthovanadate [0.7356 g Na₃VO₄ per 20 mL]
2. Adjust pH to 10 using NaOH or HCl (should be yellow in colour at pH 10)
3. Boil solution until it becomes colourless (approximately 10 minutes)
4. Cool to room temperature
5. Re-adjust pH to 10 (until the solution remains colourless and pH stabilizes at 10)
6. Store activated sodium orthovanadate as aliquots at -20°C

**** 0.5 M EGTA stock**

0.146 g EGTA per 1 mL R/O water

***** 0.5 M EDTA stock**

0.190 g EDTA per 1 mL R/O water

****** 100 mM Phenylmethylsulphonyl fluoride stock**

0.087 g phenylmethylsulfonyl fluoride in 5 mL isopropanol

Appendix E: Micro BCA™ Protein Assay Kit Working Reagent

- 25 parts Reagent A : 24 parts Reagent B : 1 part Reagent C
For 15 mL – 7.5 mL Reagent A : 7.2 mL Reagent B : 0.3 mL Reagent C

Appendix F: Loading Buffer (4X)

1. Prepare Resolving Gel

Component	10% Gel (mL)	8% Gel (mL)
R/O water	15.9	9.3
30% acrylamide	13.3	5.3

Tris-Cl (1.5M, pH 8.8)	10.0	5.0
10% SDS	0.4	0.2
10% APS	0.4	0.2
TEMED	0.016	0.012

NOTE: add APS and TEMED last

- Mix all components thoroughly and pour gel, leaving sufficient space for stacking gel and combs
 - Pipette water gently over gel solution to ensure no bubbles are present and gel polymerizes in a straight horizontal line under stacking gel
 - Allow sufficient time to polymerize (approximately 20 minutes or until a clear line is present between gel and overlaying water)
 - Pour off water, before preparing stacking gel
2. Prepare Stacking Gel

Component	5% Gel (mL)
R/O water	8.2
30% acrylamide	2.0
Tris-Cl (1M, pH 6.8)	1.5
10% SDS	0.12
10% APS	0.12
TEMED	0.012

NOTE: Add APS and TEMED last

- Mix all components thoroughly and pour gel, filling glass caste
- Insert 1.5 mm combs immediately and allow gel to polymerize
- Store in 4°C fridge wrapped in damp paper towel if not using immediately

Appendix G: 30% Acrylamide (100 mL)

- 29 g Acrylamide
- 1 g N,N' methylene bisacrylamide (dissolved in 60 mL distilled water)
- Bring volume to 100mL with distilled water

Appendix H: 1M TRIS (pH 6.8) (500 mL)

- 60.57 g TRIS
- 400 mL distilled water
- Bring volume to 500 mL once dissolved
- Adjust pH to 6.8 using either hydrochloric acid or sodium hydroxide

Appendix I: 1.5 TRIS (pH 8.8)

- 90 g TRIS
- 400 mL distilled water
- Bring volume to 500 mL once dissolved
- Adjust pH to 6.8 using either hydrochloric acid or sodium hydroxide

Appendix J: Running Buffer (10X) (2 Litres)

- 1500 mL distilled water
- 60 g TRIS
- 288 g Glycine
- Bring volume up to 2000 mL
- 20 g SDS (add last)

Appendix K: Transfer Buffer (5 Litres)

- 3500 mL distilled water
- 1000 mL methanol
- 39 mM Glycine (14.5 g)
- 38 mM TRIS (29 g)
- Top up volume to 5000 mL
- 0.0317% SDS (1.85 g) – add last

Appendix L: Blocking Solution (100 mL)

- 5% non-fat milk (5 g)

- 100 mL PBS-T

Appendix M: 1X PBS-T (1 Litre)

- Dilute 10X PBS to 1X (100 mL PBS (10X) + 900 mL distilled water)
- 2 mL 10% TWEEN solution

Appendix N: Protocol for mild stripping PVDF membranes Buffer, 1 liter

- 15 g glycine
- 1 g SDS
- 10 ml Tween20
- Adjust pH to 2.2
- Bring volume up to 1 L with R/O water.

Membrane incubation

1. Use a volume that will cover the membrane.
2. Incubate at room temperature for 5-10 minutes.
3. Discard buffer. 5-10 minutes fresh stripping buffer.
4. Discard buffer. 10 minutes PBS twice, then 5 minutes TBST twice
5. Ready for blocking stage.
6. Block membrane twice for 5 minutes with 5% non-fat milk blocking solution
7. Apply primary antibody

Appendix O: G418 (Geneticin)

- 50 mg/mL stock dissolved in water
- Dilute to 0.1 mg/mL when needed (ex. 20 μ L in one 10 mL culture flask)

Appendix P: Protein Estimation Protocol

The BSA stock was first diluted from 2.0 mg/mL to 200 µg/mL using R/O water. The stock was further diluted via serial dilution to construct a standard curve from 200 µg/mL to 1.5625 µg/mL BSA. Each unknown sample was diluted 10X with R/O water for a total volume of 150 µL in each well (15 µL sample + 135 µL R/O water). Once all standards and samples were added to the plate in duplicate, BCA reagents were mixed (25 parts reagent A : 24 parts reagent B : 1 part reagent), 150 µL of BCA reagent was added to each well and the 96-well plate was incubated for one hour at 37 °C. Absorbance was measured at 562 nm on the SpectraMax 190 Absorbance Microplate Reader (Molecular Devices) using SoftMax[®] Pro software.

Appendix Q: RNA Protocol

Total RNA was isolated from 5×10^5 PBMC with Omega Bio-tek's E.Z.N.A.[®] Total RNA Kit I with an elution volume of 40 µL. RNA concentrations were quantified with SpectraMax^R i3 spectrophotometer.

Appendix R: cDNA Synthesis kit

Components	1X Volume	10X Volume
-------------------	------------------	-------------------

5X iScript Rxn Supermix	4 µl	40 µl
iScript RT	1 µl	10 µl
RNA template	variable	variable
RNase free H ₂ O	variable	variable
Total volume	20 µl	200 µl

Appendix S: cDNA Thermocycler: Incubation Time

	Time (mins)	Temperature (°C)
1	5 mins	25 °C
2	60 mins	42 °C
3	5 mins	85 °C
4	Hold	4 °C

Appendix T: RT-PCR Primer Information

Bio Rad Product	Assay	Chromosome	Amplicon	Context Sequence
PrimerPCR SYBR Green Assay	Design:	Location:	Length	
		Mapping:	(bp):	
1. Gene Symbol: NMT1 Gene Name: N-myristoyltransferase 1 RefSeq:	Intron- spanning	Location: 17:43159068- 43163945	93	AGAAGAAAGAAA AGGCAGTGAGACA GATTCAGCCCAGGA TCAGCCTGTGAAGA

NC_000017.10, NT_010783.15 Ensembl: ENSG00000136448		Mapping 17q21.31		TGAACTCTTTGCCA GCAGAGAGGATCC AGGAAATACAGAA GGCCATTGAGCTGT TCTCAGTGGGTCAG G
2. Gene Symbol: METAP2 Gene Name: Methionyl aminopeptidase 2 RefSeq: NC_000012.11, NT_029419.12 Ensembl: ENSG00000111142	Intron- spanning	Location: 12:95879687- 95887920 Mapping 12q22	130	ATATGTGACCTGTA TCCTAATGGTGTAT TTCCCAAAGGACAA GAATGCGAATACCC ACCCACACAAGAT GGGCGAACAGCTG CTTGGAGAACTACA AGTGAAGAAAAGA AAGCATTAGATCAG GCAAGTGAAGAGA TTTGGAAATGATTTT CGAGAAGCTG
3. Gene Symbol: GAPDH Gene Name: Glyceraldehyde-3-phosphate dehydrogenase RefSeq: NC_000012.11 NG_007073.2 NT_009759.16 Ensembl: ENSG00000111640	Exonic	Location: 12:6647267- 6647413 Mapping: 12p13	117	GTATGACAACGAAT TTGGCTACAGCAAC AGGGTGGTGGACCT CATGGCCCACATGG CCTCCAAGGAGTAA GACCCCTGGACCAC CAGCCCCAGCAAG AGCACAAGAGGAA GAGAGAGACCCTC ACTGCTGGGGAGTC

				CCTGCCACAC
4. Gene Symbol: ACTB Gene Name: actin, beta RefSeq: NC_000007.13 NG_007992.1 NT_007819.17 Ensembl: ENSG00000075624	Exonic	Location: 17:43159068- 43163945 Mapping: 7p22	62	GTGCTCGATGGGGT ACTTCAGGGTGAGG ATGCCTCTCTTGCT CTGGGCCTCGTC GCCACATAGGAAT CCTTCTGACCCATG CCCACCATCA
5. Gene Symbol: RPLP0 Gene Name: Ribosomal protein, large, P0 RefSeq: NC_000012.11 NT_009775.17 Ensembl: ENSG00000089157	Exonic	Location: 12:120637113- 120637205 Mapping: 12q24.2	63	TTCTCCAGAGCTGG GTTGTTTTCCAGGT GCCCTCGGATGGCC TTGCGCATCATGGT GTTCTTGCCCATCA GCACCACAGCCTTC CCGCGAAGG

Appendix U: RT-PCR SYBR Green Mastermix

BIORAD REAGENTS	1X Volume	10X Volume
SsoAdvanced Universal supermix	7.5 µl	75 µl
Primer	0.75 µl	7.5 µl
cDNA (10ng/ µl) X 2 µl = 20ng	2 µl	20 µl
RNase free H ₂ O	4.75 µl	47.5 µl

Appendix V: Whole Blood Study: Patient's Colonoscopy/ Pathology Report

Patient	Sample	Gender/Age	Polyps	Diagnosis	CRC
1	Control 1	F/ 38	No	Normal	No
2	Control 2	F/ 70	No	Normal	No
3	Control 3	M/ 31	No	Normal	No
4	NAP 1	M/ 60	Yes (4)	Single diminutive sessile polyp (2)	No
5	NAP 2	M/ 38	Yes (2)	1. Single sessile polyp 2. Pseudopolyp	No
6	NAP 3	F/ 64	Yes (1)	Hyperplastic polyp (1)	No
7	NAP 4	F/ 65	Yes (6)	Single sessile polyp (6)	No
8	AP 1	M/ 77	Yes (6)	Tubular Adenoma (6)	No
9	AP 2	F/ 71	Yes (1)	Tubular Adenoma (1)	No
10	AP 3	F/ 49	Yes (3)	1. Tubular Adenoma (1) 2. Single sessile polyp (1) 3. Hyperplastic polyp (1)	No
11	AP 4	F/ 67	Yes (4)	1. Tubular Adenoma (1) 2. Single sessile polyp (3)	No
12	CRC 1	F/ 69	Yes (2)	Adenocarcinoma	Yes
13	CRC 2	F/ 52	Yes (3)	Adenocarcinoma	Yes
14	CRC 3	F/ 51	Yes (2)	Adenocarcinoma	Yes
15	CRC 4	M/ 73	Yes (3)	Adenocarcinoma	Yes
16	CRC 5	F/ 75	Yes (2)	Adenocarcinoma	Yes
17	CRC 6	F/ 69	Yes (1)	Adenocarcinoma	Yes
18	CRC 7	M/ 44	Yes (1)	Adenocarcinoma	Yes

Appendix W: PBMC Study: Patients' Colonoscopy/ Pathology Report

Patient	Sample	Gender/Age	Polyps	Diagnosis	CRC
1	Control 1	F/ 44	No	Normal	No
2	Control 2	F/ 54	No	Normal	No
3	Control 3	M/ 73	No	Normal	No
4	Control 4	F/ 53	No	Normal	No
5	Control 5	F/ 61	No	Normal	No
6	Control 6	M/ 27	No	Normal	No
7	Control 7	F/ 52	No	Normal	No
8	Control 8	M/ 66	No	Normal	No
9	Control	M/51	No	Normal	No
10	NAP 1	M/ 58	Yes (2)	1. Pseudopolyp 2. Hyperplastic polyp	No
11	NAP 2	M/ 73	Yes (1)	Single sessile polyp	No
12	NAP 3	M/ 38	Yes (2)	1. Single sessile polyp 2. Pseudopolyp	No
13	NAP 4	F/ 65	Yes (6)	Single sessile polyp (6)	No
14	NAP 5	M/ 53	Yes (1)	Single sessile polyp	No
15	NAP 6	M/ 67	Yes (1)	Pseudopolyp	No
16	NAP 7	F/ 67	Yes (1)	Single sessile polyp	No
17	AP 1	M/ 55	Yes (4)	1. Tubular Adenoma (1) 2. Hyperplastic polyp (3)	No
18	AP 2	F/ 72	Yes (8)	1. Tubular Adenoma (3) 2. Hyperplastic polyp (2)	No

				3. Single diminutive sessile polyp (1) 4. Diminutive sessile polyp (1) 5. Flat polyp (1)	
19	AP 3	M/ 38	Yes (4)	1. Tubular Adenoma (1) 2. Single diminutive sessile polyp (1) 3. Diminutive sessile polyp (2)	No
20	AP 4	M/ 83	Yes (9)	1. Tubular Adenoma (1) 2. Hyperplastic polyp (5) 3. Single diminutive sessile polyp (2) 4. Diminutive sessile polyp (1)	No
21	AP 5	M/ 67	Yes (1)	Tubular Adenoma (1)	No
22	AP 6	F/ 65	Yes (3)	1. Tubular Adenoma (1) 2. Single diminutive sessile polyp (1) 3. Diminutive sessile polyp (1)	No
23	CRC 1	M/ 73	Yes (3)	Adenocarcinoma	Yes
24	CRC 2	F/ 69	Yes (1)	Adenocarcinoma	Yes
25	CRC 3	F/ 71	Yes (1)	Adenocarcinoma	Yes